

Reply to Anonymous Referee #1

We would like to thank the referee for the time and the useful comments that helped to clarify important aspects of the manuscript. Our replies to the comments have been added in blue.

(1) General comments:

Ozone in the troposphere is important for the radiative budget (i.e. greenhouse gas, GHG), atmospheric chemistry (e.g. main source of hydroxyl radicals) and air quality (i.e. pollutant with negative consequences for the biosphere). Thus it is crucial to understand its evolution during the 21st century under different pathways (i.e. emission scenarios). Indeed, a key term influencing the abundance and distribution of tropospheric ozone is the stratosphere-troposphere exchange (STE). The study investigates future changes of STE following the RCP8.5 and RCP6.0 emission scenarios based on experiments of the EMAC chemistry-climate model. Projections based on chemistry-climate models are a valuable mean to probe ozone evolution associated with specific factors – i.e. such as ozone precursors, GHGs and ozone depleting substances (ODSs) – albeit significant disagreements compared to observations and between models are often found.

Overall, the study addresses relevant research questions with regard to the evolution of the STE, its drivers and the contribution of stratospheric-produced ozone to the tropospheric budget. The manuscript is technically well written. Specific comments are detailed below, which are intended to help the authors improve the paper. Briefly, I suggest more details about the “climates” (sea-surface temperatures and sea-ice concentrations, SSTs/SICs) imposed on the simulations to better interpret the comparison between the two emission scenarios considered, since they are from different models (e.g. different climate sensitivity) with consequences for ozone (e.g. chemistry and dynamics). Also, I suggest further acknowledgement to the various roles that methane plays on ozone chemistry – in the troposphere and the stratosphere – as well as its importance on the evolution of the STE. I understand in this set of simulations the effect of an enhanced Brewer-Dobson circulation and stratospheric cooling cannot be separated from the role of methane on ozone chemistry. The present study is recommended for publication after the specific and technical comments are addressed.

We thank the referee for addressing these two important aspects. We have addressed both in detail in our responses to the specific comments below, and adapted the manuscript accordingly.

(2) Specific comments:

a. The study explores how two different emission scenarios (RCP6.0 and RCP8.5) affect the stratospheric ozone mass flux into the troposphere. There is, however, an inconsistency between the SSTs/SICs used that have not been explored/detailed. In order to compare and better understand the differences in STE between these scenarios, it would be desirable to discuss how the underlying Earth System Models (ESMs) – MPI-ESM and HadGEM2-ESM – project climate. For example, the difference in global surface warming by the end of the century (2081–2099 relative to 1985–2005) between these ESMs may be as large as 1 K (higher for HadGEM2-ESM) under the RCP8.5 (see Table 3 in Friedlingstein et al., 2014 – doi.org/10.1175/JCLI-D-12-00579.1). Moreover, Fig. 11 in Jöckel et al. (2016 – doi.org/10.5194/gmd-9-1153-2016) shows that internally generated (EMAC-MPIOM) global

and annual mean SSTs for the same period but following the RCP6.0 scenario are 1 K lower compared to those projected by HadGEM2-ES. Also, the CMIP5 ensemble projects that annual mean surface air temperature anomalies for the same period under the RCP6.0 and RCP8.5 are of 2.2 ± 0.5 K and 3.7 ± 0.7 K respectively (i.e. mean difference of 1.5 K; see Table 12.2 in IPCC, 2013). Therefore, the difference between the SSTs/SICs imposed on the simulations under these emission scenarios may be relatively small, implying that ozone precursor emissions (i.e. methane) may account for a large fraction of the STE difference (i.e. rather than climate-induced).

We thank the referee for this important comment. We have addressed this issue in the revision by including the following text in Section 4:

“Note that the difference in OMF change by 2100 between the timeslice and transient simulations may not be due to the different GHG scenario alone. The HadGEM2-ES model which provided the SST/SIC distribution for the transient RCP6.0 simulation is known to have a higher climate sensitivity than the MPI-ESM which provided the SST/SICs for the EMAC timeslice runs (Andrews et al., 2012). This might lead to a somewhat stronger future SST increase, stratosphere-troposphere exchange and OMF in the transient RCP6.0 run than would arise using MPI-ESM SSTs/SICs. Hence, the differences in OMF by 2100 discussed here represent a lower boundary estimate of the expected OMF differences between the RCP6.0 and RCP8.5 scenarios.”

However, the following figure shows that the MPI-ESM RCP8.5 SSTs are clearly higher than the HadGEM2-ES RCP6.0 SSTs by the end of the century.

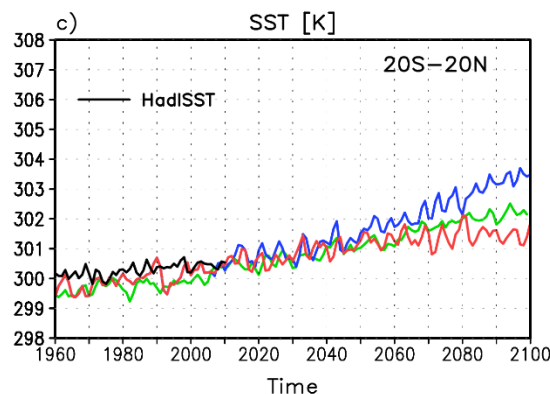


Figure 1: Annual mean SSTs from 1960 to 2100 averaged over 20°S–20°N for RCP4.5 (red) and RCP 8.5 (blue) GHG scenarios derived from MPI-ES, and for RCP6.0 derived from HadGEM2-ES (green). The RCP8.5 timeslice simulations in this study used 2095–2104 averaged SSTs from RCP8.5; the transient RCP6.0 used the transient RCP6.0 SSTs (green curve).

b. Methane is a GHG and plays various roles on ozone chemistry. Although, the authors already acknowledge the role of ozone precursors in the troposphere (i.e. methane; Page 5, lines 85–92; Page 20, lines 462–464), the effect on the stratosphere is not addressed (see below). Among other effects, it is an ozone precursor in the lower stratosphere (i.e. smog-like chemistry) and affects chlorine active/inactive partitioning, which is particularly important for polar regions under high concentrations of ODSs. An increase in methane abundances (e.g. boundary conditions) results in higher stratospheric ozone (e.g. Kawase et al., 2011 – doi.org/10.1029/2010GL046402; Revell et al., 2012 – doi.org/10.5194/acp-12-11309-2012), which will affect the stratospheric ozone mass flux into the troposphere. I guess in the GHG2100 simulation, methane is coupled to both, radiation and chemistry schemes. Therefore, the climate-induced and methane-related impacts on the STE cannot

be unambiguously separated (i.e. both included in the “GHG-induced changes”). I think this should be addressed more clearly in the manuscript and its main findings.

We included the following section to the introduction:

“Besides the temperature effect of the GHGs (mainly CO₂) on the ozone chemistry, the increasing abundances of CH₄ and N₂O also have an impact on the net production of stratospheric ozone: While higher N₂O concentrations are associated with an enhanced ozone loss in the stratosphere due to reactive nitrogen, a CH₄ increase not only causes a larger ozone loss in the lower and upper stratosphere but also leads to an increased ozone production in the lower stratosphere where it acts as an ozone precursor (e.g. Revell et al., 2012). In addition, CH₄ plays a role in polar ozone chemistry since changing CH₄ concentrations also alter the partitioning between halogen reservoir gases and activated halogen species (e.g. Nevison et al., 1999). The combined effect of the increasing GHG concentrations (including the interactions between the chemical cycles) on the net stratospheric ozone production is positive (e.g. Meul et al., 2014).”

We agree that in our simulations the climate-induced and the methane related impacts of GHG changes on STE cannot be separated, but this was not our intention but instead to distinguish between the GHG and ODS related effects on STE and tropospheric ozone change. A comment has been added in Section 2.1 for clarification.

(3) Technical comments:

Pages 1–2, lines 24–25. “. . . GHG effect on the STE change is due to circulation and stratospheric ozone changes, . . .”. Does the latter refer to stratospheric cooling and/or methane-related chemistry? Please clarify.

The abstract has been rewritten to improve clarity.

Page 1–2, Abstract. Research question (4) refers to a comparison between the emission scenarios, yet I find no reference to this in the abstract.

The abstract has been rewritten to improve clarity.

Page 4, lines 77–79. Note Banerjee et al. (2016) in their “climate” simulations did not include methane (and N₂O) in the chemistry scheme.

A respective comment has been added to the text.

Page 6, lines 111–113. The sentence reads a bit confusing – i.e. 1960–1999 period is not RCP6.0.

The sentence has been rewritten.

Page 7, lines 150–152. I guess “well-mixed GHGs” are coupled to the radiation and chemistry schemes. Please clarify, this is important to interpret the findings.

This has been clarified in the text.

Page 11, line 244. Typo: “. . . Eqation”.

Corrected

Page 11, line 246. “. . . ozone flux into the NH is larger than into the SH. . .” Is this significant?

The difference between NH maximum and SH maximum is not significant so we removed this statement from the manuscript.

Page 12, lines 252–259. Here it would be appropriate to include the STE budget term from the ACCMIP ensemble (i.e. 477 ± 96 Tg/year; mean and sdev) that informed the last (AR5) IPCC assessment report (see Table 2 in Young et al., 2013; doi.org/10.5194/acp-13-2063-2013).

The paragraph has been rewritten including information from ACCENT, ACCMIP and IPCC (2013).

Page 12, lines 259–261. Note Olsen et al. (2002) presented an influx estimate for the NH midlatitudes (e.g. see their Table 1 for further estimates).

Thank you for this note. We now use the values from IPCC (2013) based on Young et al. (2013).

Page 13, line 289. Do you mean “O3s tropospheric columns. . .”?

Yes, ‘tropospheric’ added

Page 14, lines 302–303. “low(er). . . small(er)”?

Yes, corrected

Page 14, lines 309–311. I would also include where your model lies compared to the last IPCC report. As the authors commented, there is still a relatively large uncertainty on the STE term.

A broader discussion of the STE analyses from IPCC (2013) and model intercomparisons has been included in Section 3.2

Page 15, lines 325–326. Could the “. . . unintended neglect of minor chlorine source gases. . .” account partly for the difference on ozone mass flux trends compared to Hegglin and Shepherd (2009)?

Yes, the weaker ozone depletion due to the missing minor chlorine gases could contribute to the smaller negative trend. But we don’t have the possibility to quantify this effect, so decided not to discuss this in the text.

Page 15, line 346. I would explain a bit more what the “. . . more extreme GHG emission scenario” means (i.e. climate-induced and methane-related impacts).

‘climate change- and methane-related effects’ has been included in the text.

Page 16, lines 356–359. From Fig. 5 it seems that non-linearities may not have a significant impact on the STE, and that ODS-only and GHG-only largely account for the total change (i.e. largest changes in ozone precursors are for methane).

Unfortunately, we are not able to test the impact of non-linearities but we agree that the effect is probably small.

Page 17, lines 385–389; Page 19, lines 419–420; Page 20, lines 460–462; Page 23, lines 522–524. I think the effect of methane-related chemistry on the STE and ozone should be included (assuming methane is coupled to the radiation and chemistry schemes).

We have rewritten the statement:

“The increase of F_{in} (or $O3 \times -\bar{w}^$) due to the GHG effect (Fig. 6d) is caused by an increase in the downwelling (i.e. $-\bar{w}^*$, positive for downwelling, Fig. 6e) of the BDC in the winter season with climate*

change (e.g., Sudo et al., 2003; Butchart et al., 2010; Oberländer et al., 2013) in combination with an ozone increase resulting from modified chemical production and loss rates in the stratosphere and enhanced meridional transport (Figure 6f)."

Page 18, lines 403–405. Please clarify this sentence.

We have added a new figure (Figure 7) showing the changes in the seasonal breathing term. We think that this make this section clearer.

Page 20, lines 456–457. This is a robust result from different CCMs and worth mentioning (Banerjee et al., 2017 – doi.org/10.5194/acp-2017-741; Iglesias-Suarez et al., 2017 – doi.org/10.5194/acp-2017-939).

Both manuscripts address the radiative forcing due to changes in ozone which is not a topic of this manuscript. Moreover, Iglesias-Suarez et al. (2017) is still under review. Therefore, the references have not been added.

Page 41 and 46, Figure 4 and 9. "TS RCP8.5" legend is a bit confusing since it includes year 2000 (i.e. REF2000).

We have modified the Figures. Now it is stated "TS obs+RCP8.5".

Pages 43–44, Figure 6 and 7. How is the 95 % confidence level calculated? Please explain.

The statistical significance of the future changes is tested by applying the Student's t-test. We have included this information in the text.

Page 45, Figure 8. It would be very helpful to have the annual and global mean values [DU] and [%] at the top of the figures.

Done

Reply to Anonymous Referee #2

We would like to thank the referee for the time and the useful comments that helped to clarify important aspects of the manuscript. Our replies to the comments have been added in blue.

General assessment

This manuscript investigates the role of stratosphere-troposphere exchange of ozone on the tropospheric ozone budget and its drivers – climate change and declining ODS concentrations – over the 21st century. In general, the evaluations are straightforward and the manuscript is well written. While I see some shortcomings in the experimental setup of the simulations to answer the questions posed in a clean way (see major and minor comments in the following), the study offers some new and interesting insights, which warrant publication.

Major comments

A major issue of this study results from trying to answer question 5 – How is the ratio of stratospheric ozone in the troposphere changing in the future? The problem lies in how the authors have set up their simulations to answer the questions 1-5 posed, and that they do not allow for a clean separation of the different factors (ozone precursor, ODS, CH₄, GHG effects) influencing stratosphere-troposphere exchange of ozone. As such the quantification of the relative contributions of the climate and ODS drivers seems somewhat unsatisfying, since the ratio of stratospheric to total ozone in the troposphere depends also on the mixture of the other contributing factors driving ozone in the simulations. While the study still is insightful, the shortcomings (contributions of CH₄ and ozone precursor induced ozone production) need to be discussed more thoroughly.

The major goal of our study was to investigate the impacts of future changes in both GHG increases and ODS decline between 2000 and 2100 on STE and tropospheric ozone, both for the combined effect and the separate GHG and ODS effects. The additional effect of changes in tropospheric ozone production by changes in ozone precursors was implicitly included in the simulations: In the REF2100 simulation all ozone precursors were adapted to 2100; in the GHG2100 simulation the CH₄ GHG precursor was increased to 2100 values. With this model setup the goals of our study could be addressed. To clarify the inclusion of CH₄ and precursors text has been added in Sections 2 and 4.

If I understand right, Figure 8 is meant to quantify the relative contributions of ODS decline and GHG-increases to the stratospheric ozone contribution to tropospheric ozone increases. However, I think the discussion of this Figure is not very logical. On P20 you focus first on the discussion of the relative contributions, which doesn't answer the question you pose at the beginning of the paragraph and in my eyes puts the wrong emphasis on these results. Per definition or design of your simulations, it is a given that the stratospheric contribution in the ODS-only simulation will be the main effect on tropospheric ozone levels (since nothing else is changing), so nothing surprising. The smallish regional differences can be explained by inconsistencies in boundary condition settings or internal variability of the climate system. Hence, the absolute numbers and their relative contributions to the ozone changes in the full simulation are of much more relevance and should be discussed first.

We are sorry but are not able to understand completely the referee's comment. In Fig. 9 (old Fig. 8) the left column shows from top to bottom the absolute change in the tropospheric ozone column, the absolute change in the tropospheric column of stratospheric ozone, and how much of tropospheric ozone column change is due by stratospheric ozone (in %), all that for the total forcing

by GHG and ODS changes. The middle column shows the same quantities only for GHG increase; the right column for ODS decline. We agree that in the GHG and ODS cases, change patterns are only due to the implied forcing change (and nothing else). And it is true that in the ODS run, the relative contribution from the stratosphere is very high because there is no CH₄ increase in the troposphere (hence no changed ozone production) and the effects of dynamical changes are minor (although the stratospheric contribution is not 100% everywhere). But the benefit of this figure – in our opinion - is that by comparing the change patterns of the individual forcings with those by the total forcing allows us to derive which forcing affects which region to which extent.

List of comments

Abstract: I feel that the abstract could be much improved by summarising more succinctly and more clearly the main conclusions of the manuscript. At the moment they read like a conclusions section with too much (and nevertheless not enough) detail to me. In particular L29-30 are unclear to me, since you do not explain through which mechanism GHGs lead to increased tropospheric ozone loss.

The abstract has been rewritten and hopefully clarified.

Abstract L31: The notation of ‘stratospheric column ozone in the troposphere’ is confusing to me and seems too close to the notion of the stratospheric column ozone we usually refer to (that resides in the stratosphere). Could you say ‘the column-integrated O₃s in the troposphere’ instead, or anything similar?

We have changed the notation.

P8L178ff: Appenzeller et al (1996) did only address the mass flux, not the ozone flux with their approach. It is important to note that the approach you follow is that of Hegglin and Shepherd (2009), which has to be seen as an extension of Appenzeller et al. Please add this reference to reflect this.

Reference Hegglin and Shepherd (2009) has been added to the text and the method clarified.

P4L77 Usually, scientists refer to ‘idealized model simulations’ where simplified models are used and not full-blown chemistry-climate models that hopefully are at least somewhat realistic. Suggest rephrasing here and further down (L104) as well.

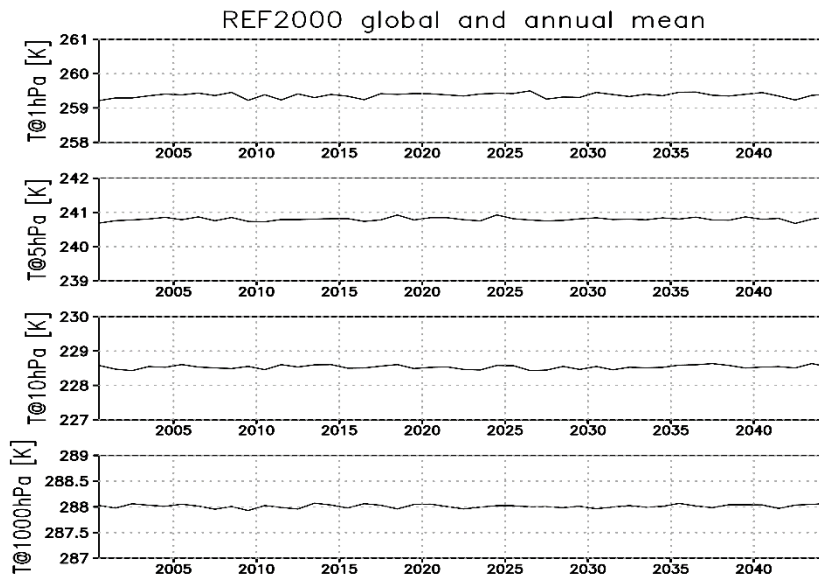
‘idealized’ not really needed here and removed at both places

P6L188 correct to ‘. . .change in the future.’

done

P7L150 Using only 5 years of spin-up seem somewhat short to me given that you would need to bring the stratosphere (with transport times around 5 years in the upper stratosphere) into an updated state. Did you make any tests to see whether the model has no remaining drifts?

Yes, we checked that there were no drifts in the analysis periods of the model runs. The figure shows as an example global annual mean temperature of the REF2000 run (the analysis period extends from model year 2005 to model year 2045; all model years are run with year 2000 conditions).



P10L209-215 The explanation of this alternative method of estimating STE is unclear to me. Did these references really use the loss of O3s and not O3 to infer STE as a residual from O3 production/loss? What additional information would this yield compared to looking at O3s change as you do here?

Yes, they use the loss of the diagnostic O3s tracer. However, since this is not relevant here we have removed this part.

P10L223ff and P11L232 It would have been more convincing to compare the model results here to actual measurements in these figures to test the realism of the transition region and stratospheric transport in EMAC. However, I realize that this may be beyond the scope of this paper and do hence not request you to do so. However, it is difficult to say what you learn from a comparison with assimilated MOPPITT data as shown in Barre et al (2013), since these data do not have the required vertical resolution to resolve the transition region. I suggest to instead compare to the ACE-FTS derived correlations in Hegglin et al. (2009) who conveniently show the CO-O3 correlations for the 30-60N latitude band in DJF (and other seasons, see their figure 7) as you have chosen in your figure. Here you see (in contrast to the Tian et al (2010) paper) that the CO-O3 correlations has a strong seasonality and latitudinal dependency. Judging by eye in the apple-to-apple comparison when using the Hegglin et al Figure, I would say EMAC is resolving the transition very well, not just reasonably well with CO values at O3=0.1, 0.5, 1,5 ppmv of around 90, 30, 17 ppbv, respectively.

The reference to the MOPPITT data has been removed and a comparison to ACE-FTS in Hegglin et al. (2009) included in the text instead. 'reasonably' has been removed.

Hegglin, M. I., C. D. Boone, G. L. Manney, K. A. Walker, A global view of the extratropical tropopause transition layer from Atmospheric Chemistry Experiment Fourier Transform Spectrometer O3, H2O, and CO, J. Geophys. Res., 114, D00B11, doi:10.1029/2008JD009984, 2009.

Reference has been added.

P11L228 The reference to Pan et al 2007 seems missing.

Pan et al. (2007) has been added in the list of references.

P12L259 IPCC (2013) has a newer compilation/assessment of STE ozone fluxes derived from different methodologies, please update to the range indicated there.

STE ozone fluxes from Table 8.1 in IPCC (2013) are used for comparison now. The section has been rewritten accordingly.

P13L276-8 It seems to me that the ozone influx from the stratosphere is larger in spring than in summer according to your results in Figure 2.

This is true for the SH, but in the NH the largest influx occurs in early summer. Text has been clarified.

P14L280 correct to '...in the SH.'

done

P14L282 again, I would prefer here '...the column-aggregated stratospheric ozone in the troposphere...'

Has been added.

P14L311 Please update this statement with respect to the IPCC 2013 results.

The reference to IPCC (2001) has been removed.

Tables 2 and 3: Please provide statistical uncertainties for your trend estimates.

The uncertainty ranges were included in Table 2 and 3. It has been added that all changes are significant on the 95% confidence level.

P16L358 See also major comment above. It seems crucial to highlight already in the methodology section that precursor emissions are not evolving in the GHG- and ODSC4 only simulations. Or did I miss this point? Can you provide an argument/estimate of the effect changes in precursor emissions could have on your results? This seems a major inconsistency in the design of your study with a potentially large effect on the amounts of ozone with stratospheric-origin in the troposphere that should be more thoroughly discussed also in the results and conclusion section. Not only are ozone precursor emissions potentially affecting the lifetime of O₃s in the troposphere, but models predict that they had a major effect on lowermost stratospheric ozone concentrations as well, which will likely influence your derived ozone fluxes through non-linear chemical reactions.

The reference simulation for the year 2100 includes changes in tropospheric precursor emissions, hence future changes in tropospheric ozone production (in addition to changes in STE). In addition, the GHG2100 simulation considering the effect of increased GHG concentrations includes increases in CH₄, i.e. the ozone precursor with the strongest trend in the RCP8.5 scenario, and consequently changes in tropospheric ozone production.

We have clarified this now by adding text in Sections 2 and 4.

P17L372-5 Reading your manuscript, I found this to be a very interesting and puzzling result, which you explain further down in more detail. However, to better envision what is going on I would appreciate to see how $-dM/dt$ changes over time in particular given that this is the second major term in determining the ozone flux into the troposphere. I hence suggest adding a figure that quantifies the LMS mass changes over the 21st century.

A new Figure 7 has been added showing dM/dt in the same format as Fig. 5. The text has been expanded to explain the seasonal variation of the seasonal breathing term for the total, GHG and ODS forcings.

P19L424-6 I do not see that O3s is transported further down in the NH than in the SH in Figure 7, rather it seems the opposite. Also, the explanation seems not really an explanation since the chemical lifetime is equally long in the SH winter than in the NH winter. Please check.

The text states: "In the SH, the abundance of stratospheric ozone increases throughout the troposphere down to the surface. More O3s seems to be transported further down than in the NH,..." "Here" has been included to avoid misunderstanding.

P20L447 correct to '... a similarly strong ...'

Done

Figure 8 caption: Please indicate that the numbers you show are changes in ozone and not absolute amounts and do not just refer to Figure 6. Using delta O3 in the figure titles would achieve the same result.

Done

Figure 9 caption L1008: did you mean 'inter-annual'?

Yes; changed.

P21L484 Sentence seems incomplete.

We removed the sentence.

P21L386-8 Another factor that needs to be discussed are tropospheric ozone precursor emissions and their effect on the tropospheric ozone burden in the RCP6.0 simulation, since this will be another confounding factor when discussing relative changes in O3s contributions to total tropospheric ozone.

The role of tropospheric ozone precursors in the RCP6.0 and RCP8.5 simulations on the relative changes in O3s contributions in the troposphere had already been discussed in the manuscript by the following sentences:

"Thus, the increase in the contribution of O3s in the future is slightly smaller in the RCP8.5 scenario than in the RCP6.0 scenario, despite the larger increase in OMF shown in Figure 2. Here, the different evolution of tropospheric ozone production in the two GHG scenarios plays a crucial role."

P22L504 correct to '... will consist of 46% ozone from ...'

Done

1 **Future changes in the stratosphere-to-troposphere ozone mass flux and the contribution**
2 **from climate change and ozone recovery**

3

4 Stefanie Meul¹, Ulrike Langematz¹, Philipp Kröger¹, Sophie Oberländer-Hayn¹, and Patrick
5 Jöckel²

6 ¹Freie Universität Berlin, Berlin, Germany

7 ²Deutsches Zentrum für Luft- und Raumfahrt (DLR) e.V., Institut für Physik der Atmosphäre,
8 Oberpfaffenhofen, Germany

9

10 **Abstract**

11 Using a state-of-the-art chemistry-climate model we investigate the future change in
12 stratosphere-troposphere exchange (STE) of ozone, the drivers of this change as well as the
13 future distribution of stratospheric ozone in the troposphere. Supplementary to previous work,
14 our focus is on changes on the monthly scale. The global mean annual influx of stratospheric
15 ozone into the troposphere is projected to increase by 53% between the years 2000 and 2100
16 under the RCP8.5 greenhouse gas scenario. The change in ozone mass flux (OMF) into the
17 troposphere is positive throughout the year with maximal increase in the summer months of the
18 respective hemispheres. Whereas in the northern hemisphere (NH) this summer maximum in
19 STE increase is a result of increasing greenhouse gas (GHG) concentrations, it is due to equal
20 contributions of decreasing levels of ozone depleting substances (ODS) and increasing GHG
21 concentrations in the southern hemisphere (SH). Here the GHG effect is dominating in the
22 winter months. A large ODS-related ozone increase in the SH stratosphere leads to a change in
23 the seasonal breathing term which results in a future decrease of the OMF into the troposphere
24 in the SH in September and October. The resulting distributions of stratospheric ozone in the

25 troposphere differ for the GHG and ODS changes because (a) ozone input occurs at different
26 regions for GHG- (midlatitudes) and ODS-changes (high latitudes), and (b) stratospheric ozone
27 is more efficiently mixed towards lower tropospheric levels in the case of ODS changes,
28 whereas tropospheric ozone loss rates grow when GHG concentrations rise. The comparison
29 between the moderate RCP6.0 and the extreme RCP8.5 emission scenarios reveals that the
30 annual global OMF trend is smaller in the moderate scenario, but the resulting change in the
31 contribution of O₃s to ozone in the troposphere is of comparable magnitude in both scenarios
32 due to the larger tropospheric ozone precursor emissions and hence ozone production in the
33 RCP8.5 scenario.

34 1. Introduction

35 Ozone (O₃) in the troposphere has two sources: photochemical production involving ozone
36 precursor species such as nitrogen oxides (NO_x), carbon monoxide (CO) and hydrocarbons
37 (e.g., methane (CH₄)) and the transport of ozone from the stratosphere into the troposphere (i.e.
38 stratosphere-troposphere exchange, STE) (IPCC, 2001). Mass can be exchanged between the
39 stratosphere and the troposphere along isentropic surfaces which intersect the tropopause in the
40 lowermost stratosphere (LMS) (Holton et al., 1995) where the chemical lifetime of ozone is
41 larger than the transport timescale. Tropopause folds in the vicinity of the polar and the
42 subtropical jets and cut-off lows are important structures for the effective transport of
43 stratospheric air masses into the troposphere because of their large displacements of the
44 tropopause on isentropic surfaces (Stohl et al., 2003). Mass exchange is also possible by slow
45 cross-isentropic transport, which is driven by diabatic cooling (Stohl et al., 2003) through the
46 large-scale vertical motion of air in the stratospheric meridional residual circulation, the
47 Brewer-Dobson circulation (BDC).

48 Earlier studies have shown that in a changing climate the mass transport from the stratosphere
49 will increase due to a strengthened BDC (e.g., Scaife and Butchart, 2001; Butchart et al.,
50 2010; Oberländer et al., 2013). Akritidis et al. (2016) found coinciding increases in the
51 frequency of tropopause folds in summer over the Eastern Mediterranean and in stratospheric
52 ozone in the lower troposphere between 1979 and 2013. In addition to changes in the ozone
53 transport from the stratosphere into the troposphere, ozone concentrations in the stratosphere
54 are expected to change. Due to declining halogen levels in the stratosphere following the
55 regulation of ozone depleting substances (ODS) by the Montreal Protocol and its
56 amendments, stratospheric ozone is projected to recover during the 21st century (e.g., WMO,
57 2014). In addition, radiative cooling of the stratosphere associated with the rising

58 concentrations of well-mixed greenhouse gases (GHG) (i.e. carbon dioxide (CO₂), nitrous
59 oxide (N₂O) and CH₄) will lead to reduced ozone loss rates and an ozone increase in the
60 stratosphere (e.g., Jonsson et al., 2004). Besides the temperature effect of the GHGs (mainly
61 CO₂) on the ozone chemistry, the increasing abundances of CH₄ and N₂O also have an impact
62 on the net production of stratospheric ozone: While higher N₂O concentrations are associated
63 with an enhanced ozone loss in the stratosphere due to reactive nitrogen, a CH₄ increase not
64 only causes a larger ozone loss in the lower and upper stratosphere but also leads to an
65 increased ozone production in the lower stratosphere where it acts as an ozone precursor (e.g.,
66 Revell et al., 2012). In addition, CH₄ plays a role in polar ozone chemistry since changing
67 CH₄ concentrations also alter the partitioning between halogen reservoir gases and activated
68 halogen species (e.g., Nevison et al., 1999). The combined effect of the increasing GHG
69 concentrations (including the interactions between the chemical cycles) on the net
70 stratospheric ozone production is positive (e.g., Meul et al., 2014).
71 -Both, the intensified stratospheric circulation, and the concurrent recovery increase of
72 stratospheric ozone are expected to lead to an increase in the ozone mass entering the
73 troposphere (e.g., Stevenson et al., 2006; Shindell et al., 2006; Hegglin and Shepherd, 2009;
74 Young et al., 2013; Banerjee et al., 2016). Previous studies with different models and
75 approaches have indicated a dominant role of stratospheric circulation changes for the
76 increased STE (e.g., Sudo et al., 2003; Zeng and Pyle, 2003; Collins et al., 2003). Also in
77 observational data, the connection between stratospheric circulation changes and tropospheric
78 ozone variations was identified (Neu et al., 2014). However for the past, Ordóñez et al. (2007)
79 showed that changes in lowermost stratospheric ozone concentrations have a larger effect on
80 the STE change than variations in cross-tropopause air mass transport. A reduced STE due to
81 stratospheric ozone depletion in the past was found by Shindell et al. (2006) to offset more
82 than half of the tropospheric ozone increase since preindustrial times. The influence of

83 stratospheric ozone recovery on STE in the future was reported by Zeng et al. (2010) who
84 showed that in the Southern Hemisphere (SH) during winter stratospheric ozone increase and
85 climate change have a nearly equal contribution to the increase in surface ozone under the
86 A1B scenario. More recently, the drivers of future STE changes have been analysed by
87 Banerjee et al. (2016) in ~~idealized~~ model simulations. Neglecting the impact of methane and
88 N₂O. They find that ODS and climate change under the RCP8.5 scenario contribute about
89 equally to the annual global STE increase between 2000 and 2100.

90 Rising GHG concentrations, however, do not only affect the stratospheric circulation and
91 chemistry. In the troposphere, GHG-induced warming increases the water vapour content and
92 thus tropospheric ozone destruction (e.g., Johnson et al., 1999). This results in a decrease of
93 chemical ozone lifetimes (e.g., Zeng et al., 2010; Banerjee et al., 2016) which means that the
94 distribution and the burden of stratospheric ozone entering the troposphere are also altered.

95 In addition to a changing amount of stratospheric ozone in the troposphere, changing future
96 emissions of ozone precursor species will affect the local ozone production in the troposphere
97 (e.g. Monks et al., 2009). Large differences exist in the temporal evolution of the emissions
98 between the Representative Concentration Pathways (RCP) for the radiative forcing of 6.0
99 W/m² and 8.5 W/m² (Meinshausen et al., 2011), especially for CH₄. This will result in a larger
100 ozone production under the RCP8.5 scenario at the end of the 21st century compared to the
101 RCP6.0 scenario. As a consequence, the importance of stratospheric ozone in the troposphere
102 in the future will depend on the net tropospheric chemical ozone production.

103 Most studies addressing the question of future STE changes and their role for tropospheric
104 ozone trends focus on the annual and global integrated fluxes. Hegglin and Shepherd (2009)
105 showed also the annual cycle of the ~~ozone mass flux~~ OMF derived from a boxmodel approach
106 introduced by Appenzeller et al. (1996). In their model simulation, the maximum ozone flux
107 occurs in spring in the SH and ~~Northern Hemisphere~~ (NH) for the 1960 to 1970 mean. In the

108 future (2090-2100), the peak is shifted towards late spring/early summer in the NH and towards
109 winter in the SH. As Roelofs and Lelieveld (1997) reported, the seasonal timing of the input of
110 stratospheric ozone into the troposphere is relevant for potential mixing of stratospheric ozone
111 towards the surface, since in summer the ozone loss rate is larger than in winter. This means
112 that the future distribution of stratospheric ozone in the troposphere depends not only on the
113 overall increase on OMF, but also on the seasonality of the input.

114 The aim of our study is therefore, to quantify the future changes of STE in idealized simulations
115 with a chemistry-climate model (CCM) under the most extreme RCP8.5 scenario for the annual
116 and monthly means. We identify the changes in the seasonal cycle of STE due to the projected
117 increase in GHGs and decline in ODS, i.e. the associated stratospheric ozone recovery.
118 Furthermore, we analyse the resulting changes in the distribution of stratospheric ozone in the
119 troposphere, using comprehensive stratospheric and tropospheric chemistry. We thus—and
120 therefore—considering the full range of changes in chemical loss and production caused by GHG
121 or ODS changes. By analyzing The additional analysis with an additional—transient
122 simulation run under the RCP6.0 scenario we are able allows us on the one hand to study
123 the past changes between 1960 and 1999 and on the other hand to compare assess the different
124 effects of a moderate and a strongtwo different GHG scenarios and their effect on the future
125 OMF and trends of stratospheric ozone trends in the troposphere.

126 In this study we want to address the following research questions:

- 127 (1) How will the stratosphere-to-troposphere ~~ozone mass flux~~OMF change in the future?
- 128 (2) What are the major drivers of the future changes in the stratosphere-to-troposphere ~~ozone~~
129 ~~mass flux~~OMF?
- 130 (3) Will the seasonality of the STE change in the future?
- 131 (4) How will the GHG emission scenarios affect the ~~ozone mass flux~~OMF into the troposphere?
- 132 (5) How is the ratio of stratospheric ozone in the troposphere changed in the future?

133 The study is structured as followed: First the model and the experimental set-up used for the
134 simulations are described as well as the methodology for calculating the ~~ozone mass flux~~OMF
135 from the stratosphere to the troposphere (Section 2). In Section 3 we show the climatological
136 mean state of the year 2000 simulation for a basic evaluation. Results of mass flux changes and
137 changes in the distribution of stratospheric ozone in the troposphere are shown in Section 4
138 followed by the attribution analysis in Section 5. The results are summarized in Section 6.

139

140 **2. Model experiments and methods**

141 **2.1 Model experiments**

142 In this study we applied the EMAC (ECHAM/MESSy Atmospheric Chemistry) CCM version
143 described by Jöckel et al. (2016) in the T42L47MA configuration, i.e. with 47 model layers and
144 a horizontal resolution of $2.8^\circ \times 2.8^\circ$. EMAC is a numerical chemistry and climate simulation
145 system that includes submodels describing tropospheric and middle atmosphere processes and
146 their interaction with oceans, land and human influences (Jöckel et al., 2016). It uses the second
147 version of the Modular Earth Submodel System (MESSy2) to link multi-institutional computer
148 codes. The core atmospheric model is the 5th-generation European Centre Hamburg general
149 circulation model (ECHAM5) (Roeckner et al., 2006). The atmospheric chemistry is calculated
150 using the submodule MECCA (Module Efficiently Calculating the Chemistry of the
151 Atmosphere; revised version by Sander et al., 2011a). The gas-phase rate coefficients follow
152 the latest recommendations of JPL (Sander et al., 2011b). For heterogeneous reactions in the
153 stratosphere the rate coefficients are calculated with the submodel MSBM (Multi-phase
154 Stratospheric Box Model) which also returns the parameters (e.g., number densities, surface
155 areas) of the sulfuric acid aerosols and the polar stratospheric cloud (PSC) particles.

156 To quantify the impact of increasing GHG concentrations and of declining stratospheric

157 halogen levels on the net ~~ozone mass flux~~OMF from the stratosphere into the troposphere, we
158 performed four experiments in timeslice mode, i.e. with non-varying boundary conditions from
159 year to year, but including a seasonal cycle. In addition to reference simulations for the years
160 2000 and 2100, one sensitivity simulation for GHG increase only and one for ODS decrease
161 only have been set up. Each timeslice simulation has been integrated over 40 years following 5
162 years of spin-up time. Future surface concentrations of the well-mixed GHGs (CO₂, N₂O, CH₄)
163 are prescribed according to the extreme RCP8.5 scenario (Meinshausen et al., 2011) in order to
164 reveal the upper boundary of the anticipated future changes. They are coupled to both the
165 radiation and chemistry schemes of the model. The changes in tropospheric ozone precursor
166 species (such as nitrogen monoxide (NO), carbon monoxide (CO), CH₄ and non-methane
167 volatile organic compounds (NMVOCs) also follow the RCP8.5 emission scenario and are
168 included in the reference simulation for the year 2100. Since CH₄ acts as both a GHG and
169 tropospheric ozone precursor, a clear separation of the effects by prescribing the surface
170 boundary conditions in a model run is not possible. Therefore, for the GHG sensitivity
171 simulation the non-methane precursor compounds are fixed at the year 2000 level (see Table 2)
172 whereas CH₄ is increasing. Although the RCP scenarios project the surface emissions of NO_x,
173 CO and NMVOCs in the year 2100 to be lower than in the year 2000, the strong increase in
174 CH₄ concentrations (more than doubling in the RCP8.5) will lead to an increased tropospheric
175 ozone production by the end of the 21st century which is attributed to the GHG change in this
176 study.

177 -The estimated decline of ODS as a consequence of the successful regulation of halogen
178 containing species in the Montreal Protocol and its amendments is given by the boundary
179 conditions following the A1 scenario in WMO (2011). Note that due to an unintended neglect
180 of minor chlorine source gases CFC-113, CFC-144, CFC-155 as well as HCFC-22, HCFC-
181 141b and HCFC-142b, stratospheric chlorine levels in the year 2000 are underestimated by

182 about 10%.

183 The quasi-biennial oscillation (QBO) of tropical winds in the stratosphere is nudged to
184 observations following Giorgetta and Bengtsson (1999). Solar variability like the 11-year solar
185 cycle is not included, instead solar mean conditions of solar cycle number 22 are prescribed.
186 The sea surface temperature (SST) and sea ice concentration (SIC) fields are prescribed as 10-
187 year averages around the respective years using the output from a transient simulation with the
188 coupled atmosphere ocean model MPI-ESM (Max-Planck-Institute Earth System Model;
189 Giorgetta et al., 2013; Schmidt et al., 2013) for the RCP8.5 scenario. Using multi-year averages
190 reduces the inter-annual variability of the SSTs, but ensures quasi neutral conditions of the El
191 Niño Southern Oscillation (ENSO). An overview of the boundary conditions in the four
192 simulations is given in Table 1. [The chosen setup of the simulations allows us to separate the](#)
193 [combined effect of the CO₂, N₂O and CH₄ increase from the ODS effect on the future OMF. It](#)
194 [has to be noted that the GHG-induced changes in this study include all GHG-related effects on](#)
195 [stratospheric chemistry and dynamics, and the contributions from GHG-induced climate change](#)
196 [cannot be separated from the impact of CH₄ and N₂O related changes in the ozone chemistry.](#)

197 To show the temporal evolution of the changes and to compare the effects for different GHG
198 scenarios we also analyse the model output from the transient simulation RC2-base-05 of the
199 Earth System Chemistry integrated Modelling (ESCiMo) project (Jöckel et al., 2016) which has
200 been integrated according to the RCP6.0 scenario from 1960 to 2100 following a 10-year spin-
201 up. The SST and SIC fields for the RCP6.0 scenario are prescribed from the Hadley Centre
202 Global Environment Model version 2 - Earth System (HadGEM2-ES) Model (Collins et al.,
203 2011; Martin et al., 2011). The boundary conditions for this simulation are given in Table 1.
204 More detailed information of this simulation can be found in Jöckel et al. (2016). [Note that](#)
205 [consistent SSTs/SICs from a MPI-ESM RCP6.0 simulation were not available. Potential effects](#)

206 of the different SST datasets are discussed in section 4. It has also to be noted, that the
207 stratospheric ozone loss in the past is underestimated in this simulation, which affects the trends
208 in ~~ozone mass flux~~OMF.

209 **2.2 Methods**

210 To quantify the net ~~ozone mass flux~~OMF from the stratosphere into the troposphere we
211 ~~follow~~apply the ~~boxmodel~~ approach described by Hegglin and Shepherd (2009) which is an
212 extension to the boxmodel approach by Appenzeller et al. (1996). ~~They~~Appenzeller et al. (1996)
213 described the hemispheric net mass transport in a simple model which consists of three regions
214 (i.e. boxes), the troposphere, the 'lowermost stratosphere' (LMS) and the 'overworld'. The LMS
215 is the region where isentropic surfaces intersect the tropopause. Thus mass can be exchanged
216 between the stratosphere and the troposphere along such isentropic surfaces. Above the LMS,
217 often referred to as the overworld according to Holton et al. (1995), the isentropic surfaces lie
218 entirely in the stratosphere and mass exchange is only possible by cross-isentropic transport,
219 which is carried out by the large-scale meridional circulation in the stratosphere (BDC). Due to
220 mass continuity, a mass flux from the overworld into the LMS (F_{in}) must be balanced by a mass
221 flux out of the LMS (F_{out}) and/or mass change (dM/dt) in the LMS:

$$222 \quad F_{in} = F_{out} + dM/dt \quad (1).$$

223 In our study we use the 91 hPa surface (nearest pressure level of the model output to 100 hPa)
224 as upper boundary for the LMS boxmodel and the model tropopause (a combination of the
225 thermal tropopause in the tropics and the dynamical tropopause in the extratropics) as lower
226 boundary, analogously to Hegglin and Shepherd (2009). Thus, M in Equation 1 is the total
227 ozone mass between these boundaries, and dM/dt is the monthly change of M . F_{in} is calculated
228 for each hemisphere as the area-weighted integral of the product of the monthly zonal mean
229 ozone concentration and the negative of the monthly mean residual vertical velocity ($-\bar{w}^*$) at 91

230 hPa at each gridpoint. Since, by definition, the vertical velocity is positive for upward and
231 negative for downward motion, \bar{w}^* is multiplied by the factor -1 in order to get positive values
232 for the downward ~~ozone mass flux~~OMF into the troposphere. Finally, F_{out} is calculated as
233 residual. It has to be noted that with this methodology it is not possible to study the transport
234 pathways. The use of the 91 hPa surface as upper boundary instead of 100 hPa leads to slightly
235 lower values of the resulting ~~ozone mass flux~~OMF (< 2% in the REF2000 simulation,
236 estimation based on linear interpolation between the two model pressure surfaces surrounding
237 100 hPa).

238 To distinguish ozone with stratospheric origin (O3s) and ozone produced in the troposphere
239 (O3t) we use a diagnostic tracer O3s (Roelofs and Lelieveld, 1997; Collins et al., 2003; Jöckel
240 et al., 2016). This tracer is reset in each model time step (by nudging with a relaxation time
241 equaling the model time step length) to the interactive ozone above the model tropopause. In
242 the troposphere, the chemical production of O3s is omitted while the sinks of O3s, i.e. chemical
243 loss and dry deposition, are considered in the same way as for O3. ~~The loss of O3s (LO3s) plus~~
244 ~~the dry deposition have been used as a qualitative measure of STE in earlier studies (e.g.,~~
245 ~~Roelofs and Lelieveld, 1997; Jöckel et al., 2006). However, in our study this different method~~
246 ~~of STE estimation was not applied since the output of dry deposition for the O3s tracer was not~~
247 ~~available. Also, LO3s is not only affected by changes in ozone flux but also by changes in~~
248 ~~tropospheric ozone chemistry due to the prescribed forcings, potentially leading to differences~~
249 ~~in the derived STE. The statistical significance of the future changes is tested by applying the~~
250 Student's t-test.

251

252 3. Equilibrium state of the year 2000 (REF2000)

253 Before we estimate the future change in ~~ozone mass flux~~OMF into the troposphere, the present-
254 day equilibrium state is analysed to ensure that the important mixing processes and tracer
255 distributions are represented realistically in the EMAC simulations. An effective method to
256 investigate STE and mixing processes in the LMS are tracer-tracer correlations.

257 3.1 Tracer-tracer correlations from scatter plots

258 Fischer et al. (2000) introduced the O₃-CO correlations for aircraft in situ measurements to
259 analyse the chemical transition between the stratosphere and troposphere and the mixing
260 processes in the UTLS. Due to the sharp gradients with high CO (low O₃) values in the upper
261 troposphere and low CO (high O₃) values in the lower stratosphere, the O₃-CO scatter plot has
262 a characteristic L-shape in the UTLS (e.g., Fischer et al., 2000; Tian et al., 2010; Barré et al.,
263 2013). Pan et al. (2007) distinguish the stratospheric branch and the tropospheric branch with a
264 quasi linear relation between O₃ and CO and a transition region in between characterized by
265 non-linear behavior. Figure 1 (top) shows the O₃-CO scatter plot for the REF2000 simulation
266 in the northern ~~middle mid~~ latitudes. Compared to the ~~correlations results~~ shown by Fischer et
267 al. (2000) (~~derived from~~ aircraft measurements) and ~~by Hegglin et al. (2009) (derived from~~
268 ~~ACE-FTS measurements) Barré et al. (2013) for measurements and model data,~~ we find that
269 the L-shape of the correlation is captured ~~reasonably~~ well by the EMAC timeslice simulation.

270 The shape of the O₃-N₂O scatter plot (Figure 1, bottom) with a full stratosphere coverage results
271 from the negative vertical gradient in N₂O and the O₃ maximum in the stratosphere: The
272 correlation is negative below the ozone maximum and positive above. The fan-shaped structure
273 is due to the horizontal gradient with higher O₃ and N₂O values in the tropics than in the extra-
274 tropics. The model result is in qualitative agreement with O₃-N₂O scatter plots for ACE
275 measurements shown by Hegglin and Shepherd (2007).

276 This comparison indicates that the dynamical and chemical processes in the transition region
277 between the troposphere and stratosphere are realistic in the EMAC timeslice simulations and
278 allows us to assess the future changes.

279 **3.2 Ozone mass flux (OMF)**

280 The annual cycle of the ~~ozone mass flux~~OMF into the troposphere (F_{out} , calculated according
281 Equation 1) for the year 2000 reference simulation is shown in Figure 2a, integrated globally
282 and over the NH and SH respectively. The ~~ozone mass flux~~OMF into the NH ~~is larger than into~~
283 ~~the SH and~~ has its peak in early summer (June), whereas in the SH the maximum ~~ozone mass~~
284 ~~flux~~OMF is found in spring (October). The annual cycle in the EMAC REF2000 simulation is
285 comparable to the results of Hegglin and Shepherd (2009) for the period 1960 to 1970, but with
286 a less pronounced peak in the NH spring in EMAC.

287 Integrated over all months, the ~~ozone mass flux~~OMF in the EMAC REF2000 timeslice
288 ~~simulation~~ reaches 390 ± 187 Tg per year in the NH, 322 ± 165 Tg per year in the SH and 712
289 ± 264 Tg per year globally. ~~Compared to estimates derived from observations (540 ± 140 Tg~~
290 ~~per year; Olsen et al., 2001; Wild, 2007), the global OMF is slightly overestimated in EMAC,~~
291 ~~however, within the range of 340 – 1440 Tg per year given by Wild (2007) for a number of~~
292 ~~models. The global ozone mass flux~~The STE OMF in EMAC hits the upper boundary of the
293 ~~ozone mass flux~~OMF derived from ~~the Atmospheric Composition Change: the European~~
294 ~~Network of excellence (ACCENT) tropospheric model intercomparisons for the year 2000 (552~~
295 ~~± 168 Tg per year) (for the year 2000 (552 ± 168 Tg/year; Stevenson et al., 2006), while and is~~
296 ~~larger than the ozone mass flux reported by Hegglin and Shepherd (2009) (655 ± 5 Tg/year),~~
297 ~~which was derived by averaging the 1995 to 2005 period of a transient simulation with a middle~~
298 ~~atmosphere resolving CCM, or by Young et al. (2013) (477 ± 96 Tg/yr) who estimated the~~
299 ~~mean net influx of STE ozone from the stratosphere to the troposphere-OMF from six models~~

300 of the Atmospheric Chemistry and Climate Model Intercomparison Project (ACCMIP) was
301 lower (477 ± 96 Tg per year; Young et al., 2013). The estimated STE OMFs generally show a
302 large range as they strongly depend on various factors, such as the prescribed ozone precursors,
303 the horizontal and vertical resolution of the applied models, the definition of the tropopause, or
304 the degree of chemical processes considered in the models. Hegglin and Shepherd (2009), using
305 a middle atmosphere resolving CCM with full chemistry – comparable in complexity to the
306 EMAC CCM used in this study – derived a global STE ozone flux of 655 ± 5 Tg per year,
307 averaged over the 1995 to 2005 period of a transient simulation. However, the ozone mass flux
308 in the REF2000 simulation lies in the range of 340–930 Tg/year given by Collins et al. (2000)
309 for a range of models and agrees well with the ozone mass flux of 770 ± 400 Tg/year given in
310 IPCC (2001). Compared to estimates derived from observations (500 ± 140 Tg/year; Olsen et
311 al., 2002), the ozone mass flux in the EMAC timeslice simulation is slightly overestimated.

312 To better understand the changes in the calculated ~~ozone mass flux~~OMF ($F_{\text{out}} = F_{\text{in}} - dM/dt$),
313 we analyse the climatological annual cycle of the two ~~ozone mass flux~~OMF components, F_{in} at
314 91 hPa (Figure 2b) and $-dM/dt$ (Figure 2c). The ~~ozone mass flux~~OMF across the 91 hPa
315 pressure level is controlled by the seasonality of the BDC with the maximum (ozone) net mass
316 transport flux into the LMS in the winter hemisphere and a hemispherically asymmetric strength
317 (Figure 2b). The ozone distribution in the stratosphere (see also Figure 3a) with low columns
318 in the tropics and high columns in the middle and high latitudes also reflects the structure of the
319 stratospheric meridional circulation.

320 The seasonal breathing of the LMS (Figure 2c) leads to a shift of the maximum high ozone
321 mass fluxOMF phase from winter to spring and early summer (which is consistent with Hegglin
322 and Shepherd, 2009) and of the low OMF phase from summer to autumn. The amplitude of the

323 seasonal cycle in $-dM/dt$ is slightly larger in the NH than in the SH which dampens the
324 amplitude of the ~~ozone mass flux~~OMF in the NH.

325 The timing of the maximum ~~ozone mass flux~~OMF into the troposphere is relevant for the
326 resulting downward mixing since the chemical lifetime of tropospheric ozone in the mid- and
327 high latitudes has a pronounced seasonal cycle with short lifetimes in the summer and relatively
328 long lifetimes in winter and spring. This means that ozone can be mixed more efficiently with
329 tropospheric air masses in winter and spring (Roelofs and Lelieveld, 1997) although the ozone
330 influx from the stratosphere is smaller in northern early spring than in summer.

331 In the next section we analyse the abundance of stratospheric ozone with stratospheric origin
332 (O3s) in the troposphere for June (Figure 3), when the ~~ozone mass flux~~OMF is maximal in the
333 NH and minimal in the SH (Figure 2a).

334 **3.3 Stratospheric ozone in the troposphere**

335 ~~In the troposphere, the columns of ozone originating from the stratosphere (The column-~~
336 ~~aggregated stratospheric ozone in the troposphere~~ (Figure 3b) reaches a maximum of 30 DU
337 around 30° in both hemispheres and a minimum in the tropics (3-6 DU over Indonesia) and the
338 southern high latitudes. The low values in the tropics presumably result from very short ozone
339 lifetimes near the surface as the high insolation and high water vapour concentrations in the
340 intertropical convergence zone (ITCZ) form a strong sink for tropospheric ozone in the
341 troposphere (Roelofs and Lelieveld, 1997). In addition, the downward transport of stratospheric
342 ozone in the tropics is very small due to the upward branch of the BDC in this region. The high
343 tropospheric O3s columns in the subtropics result from high abundances of stratospheric ozone
344 in the upper troposphere, especially in the NH subtropics, which is evident in Figure 3c. Here,
345 ozone entering the troposphere through tropopause folds is efficiently transported to lower
346 altitudes in the downward branch of the Hadley cell (Roelofs and Lelieveld, 1997) resulting in

347 relatively high O₃s levels in the middle troposphere around 30°N. The O₃s mixing ratios
348 decrease with lower altitude and reach their minimum near the surface, with the smallest values
349 in the tropics and the NH, since ozone loss is largest in summer (Figure 3d). However, ozone
350 originating from the stratosphere is also found down to the lower troposphere in the extra-
351 tropics. This may be caused by events when stratospheric air penetrates deep into the
352 troposphere and affects also lower levels (e.g., Škerlak et al., 2014).

353 The contribution of O₃s to ~~ozone~~ O₃ (=O₃s+O₃t) is in the range between 20-% in the tropics
354 and the NH lower troposphere and up to 40-% in the middle troposphere (500 hPa) in the NH.
355 In the SH, the relative contribution of O₃s to O₃ is larger (50-60-% near the surface and more
356 than 60-% at 500 hPa at high latitudes). This is caused by lower chemical loss of O₃s in winter
357 (Figure 3d) in combination with smaller chemical production of tropospheric ozone in this
358 season. In SH summer this pattern is reversed (not shown), however, with a slightly larger
359 contribution of O₃s near the SH surface (20-30-%) compared to NH summer. This is possibly
360 related to the lower local photochemical ozone production in the SH due to reduced emissions
361 and abundances of tropospheric ozone precursor species.

362 In summary, we have found realistic tracer distributions in the tropopause region of the EMAC
363 reference simulation for the year 2000. The ~~ozone mass flux~~OMF appears to be overestimated
364 compared to observations and other model studies, ~~while lying within the range estimated in~~
365 ~~IPCC (2001).~~ However, ~~G~~ given the large uncertainties for estimates from observational data
366 and the range of different model types, the ~~ozone mass flux~~OMF in EMAC can be regarded as
367 reasonable. The results indicate that the important processes determining the STE are
368 sufficiently well reproduced by EMAC, which allows us to study in the next section the past
369 and future changes of the ~~ozone mass flux~~OMF as well as the contributions from GHG and
370 ODS changes.

372 4. Past and future changes in ~~ozone mass flux~~OMF into the troposphere

373 Changes in the input of stratospheric ozone into the troposphere can be caused by changes in
374 the dynamical processes and/or by the amount of ozone that is available for transport in the
375 stratosphere. Thus, not only GHG concentrations may have an impact on the stratosphere-to-
376 troposphere transport but also the development of the ODS. The ~~temporal~~-evolution ~~between~~
377 ~~1960 and 2099~~ of the integrated ~~ozone mass flux~~OMF ~~between 1960 and 2099~~ for the RCP6.0
378 simulation, which includes ~~both~~, the observed, and projected ODS and GHG changes as well
379 as the increase in tropospheric ozone precursor concentrations, is shown in Figure 4. In the past
380 (1960-1999), the integrated ~~ozone mass flux~~OMF exhibits a negative trend in both hemispheres
381 with a larger change of -1.4-% per decade in the SH which is in qualitative agreement but
382 smaller than the trend (-2.3-% per decade) found by Hegglin and Shepherd (2009) between
383 1965 and 2000. Zeng et al. (2010) showed that this negative trend is associated with the ODS-
384 induced ozone loss in the stratosphere which is most prominent in the southern polar region in
385 spring. Between 2000 and 2099 the ~~ozone mass flux~~OMF is projected to increase globally by
386 4.2-% per decade. Again, the change in the SH (4.9-% per decade) is slightly larger than in the
387 NH (3.7-% per decade). This increase may be ~~the consequence of~~ascribed to different forcings:
388 (1) the regulations of ODS emissions lead to a decline of chlorine in the stratosphere and
389 increasing stratospheric ozone levels; (2) the increasing GHG concentrations alter the
390 temperature structure of the atmosphere and intensify the large-scale mass transport in the
391 stratosphere, and (3) the radiative cooling of the stratosphere due to increasing GHG
392 concentrations slows chemical loss reactions, which increases the ozone amount in the
393 stratosphere. To understand the impact of ODS and GHG changes on the ~~ozone mass flux~~OMF
394 in more detail, we further analyse the sensitivity simulations following the RCP8.5 scenario.

395 For comparison the reference timeslice simulations for the years 2000 and 2100 are included in
396 Figure 4. The 1995-2004 average in the RCP6.0 simulation gives an ~~ozone mass flux~~OMF of
397 688 ± 24 Tg per /year which is slightly lower than in the timeslice simulation for 2000, but
398 within the range of two standard deviations of the REF2000 simulation. This difference might
399 be due to the reduced variability in the timeslice simulation compared to the transient one (see
400 Section 2), and/or due to the different SST/SIC fields used in the simulations. However, the
401 results of the model simulations are in relatively good agreement.

402 In the future, the ~~ozone mass flux~~OMF is clearly larger in the timeslice simulations than in the
403 transient simulation due to the climate change- and methane-related effects of the more extreme
404 GHG emission scenario (RCP8.5 compared to RCP6.0). The integrated ~~ozone mass flux~~OMF
405 reaches 598 ± 29 Tg per /year in the NH, 490 ± 23 Tg per /year in the SH and 1088 ± 43 Tg per
406 /year for the global sum. This corresponds to a relative increase of 5.3%, 5.2% and 5.3-% /per
407 decade, respectively (see also Table 2). Thus, ~~in contrast to while in the transient~~ RCP6.0
408 ~~scenario~~imulation, the ~~future ozone mass flux~~OMF increase by the end of the century is stronger
409 change in the SH than in the NH due to the prevailing impact of stratospheric ozone recovery in
410 the SH, OMF increases are of similar magnitude in both hemispheres for the RCP8.5 GHG
411 scenario. This is due to the growing role of an increased BDC in the RCP8.5 scenario which
412 has a stronger impact in the NH~~timeslice simulations is similar in the NH and in the SH. Note~~
413 that the difference in OMF change by 2100 between the timeslice and transient simulations may
414 not be due to the different GHG scenario alone. The HadGEM2-ES model which provided the
415 SST/SIC distribution for the transient RCP6.0 simulation is known to have a higher climate
416 sensitivity than the MPI-ESM which provided the SST/SICs for the EMAC timeslice runs
417 (Andrews et al., 2012). This might lead to a somewhat stronger future SST increase, STE, and
418 OMF in the transient RCP6.0 run than would arise using MPI-ESM SSTs/SICs. Hence, the

419 differences in OMF by 2100 discussed here represent a lower boundary estimate of the expected
420 OMF differences between the RCP6.0 and RCP8.5 scenarios.

421

422 **5. Attribution of future changes in ~~ozone mass flux~~OMF to climate change**

423 Figure 5 shows the monthly changes of the ~~ozone mass flux~~OMF for the sensitivity simulations,
424 i.e. for the total change between 2000 and 2100 due to all forcings and the ~~contributions~~
425 ~~changes resulting~~ from GHG and ODS changes ~~only~~. It has to be noted that the changes due to
426 GHGs and ODS do not necessarily sum up to the total change ~~due to because of~~ non-linear
427 interactions and ~~due to the fact that~~ the ~~missing~~ change in ~~non-methane~~ tropospheric ozone
428 precursor species ~~in the ODS only and GHG only is only included in the reference~~ simulation
429 ~~for 2100s~~ (see Table 1). ~~However, in the RCP8.5 scenario the largest changes in ozone~~
430 ~~precursors are for methane which are included in the GHG signal.~~

431 ~~Nevertheless, the effect of the projected increase in tropospheric ozone precursor concentrations~~
432 ~~on the ~~ozone mass flux~~OMF change between 2000 and 2100 ~~can'tcannot~~ be unambiguously~~
433 ~~separated from the total change in this study. This is also due to the impact of the non-methane~~
434 ~~ozone precursors on ozone production in the lower stratosphere and the tropospheric ozone loss~~
435 ~~which can affect the OMF as well as the O3s distribution in the troposphere. While all these~~
436 ~~interactions are taken into account in the future reference simulation, the objective of the~~
437 ~~sensitivity runs of this study is to simplify the complexity and to focus on the changes driven by~~
438 ~~the well-mixed GHGs and the ODSs.~~

439 ~~Furthermore, all results shown for the GHG-induced signal in the OMF consist of both the~~
440 ~~contribution from a strengthened BDC and the chemically driven (climate and CH₄ related)~~
441 ~~increase in stratospheric ozone available for downward transport.~~

442 The change in ~~ozone mass fluxOMF~~ between 2000 and 2100 due to all forcings ([Figure 5](#), top
443 row) is positive throughout the year with maximal increases in the summer months of the
444 respective hemispheres by up to 32 Tg ~~per /month~~ (75-%) in the NH and 19 Tg ~~per /month~~ (68
445 %) in the SH. The GHG ([Figure 5](#), middle row) and ODS ([Figure 5](#), bottom row) induced
446 changes clearly indicate the dominant role of rising GHG concentrations for the future ~~ozone~~
447 ~~mass fluxOMF~~ change in the NH, ~~explaining 80 to 95 % of the total change~~. In the NH, tThe
448 GHG-related ~~ozone mass fluxOMF~~ increase ~~in the NH~~ is maximal in June and July, slightly
449 shifting the peak in the annual cycle to later in summer which is consistent with the findings by
450 Hegglin and Shepherd (2009) ~~for the total change between the 1960-1970 and 2090-2100~~
451 ~~means~~. The ODS decrease, however, leads only to small positive and (not significant) negative
452 changes in the NH.

453 In the SH, the GHG-induced increase dominates the ~~ozone mass fluxOMF~~ change in winter
454 and spring, ~~but while in summer~~ the ODS-related increase of the ~~ozone mass fluxOMF~~
455 contributes ~~up to 50 %~~ nearly equally to the total change in ~~the SH~~ summer. A significant
456 reduction of ~~ozone mass fluxOMF~~ is found from August to October in the SH due to the ODS
457 change. This causes a shift of the SH maximum ozone flux from October to December/January
458 and is in contrast to the results by Hegglin and Shepherd (2009) who found the maximum SH
459 ~~ozone mass fluxOMF~~ in the future (2090-2100) to occur in August.

460 Overall we find that the GHG-induced changes will determine the positive trend of the ~~ozone~~
461 ~~mass fluxOMF~~ in the NH, while in the SH both ODS and GHG changes affect the trend and the
462 seasonality of the future ~~ozone mass fluxOMF~~ into the troposphere.

463 To identify the processes behind the ODS- and GHG-induced changes, we analyse the changes
464 of the two ~~ozone mass fluxOMF~~ components, i.e. F_{in} and the seasonal breathing term. We find
465 that the integrated F_{in} will increase in the future throughout the year in both hemispheres and

466 for both external forcings (not shown). [To give a more detailed picture](#) Figure 6 shows in the
467 top row the latitudinal distribution of the product of ozone concentration and $-\bar{w}^*$ at 91 hPa,
468 which equals F_{in} , when integrated over all latitudes. The two components of F_{in} , $-\bar{w}^*$ and the
469 ozone concentration, are shown separately in the middle and bottom rows of Figure 6,
470 respectively. The increase of F_{in} (or $O_3 \times -\bar{w}^*$) due to the GHG effect (Figure 6d) is caused by
471 an increase in the downwelling (i.e. $-\bar{w}^*$, positive for downwelling, Figure 6e) of the BDC in
472 the winter season with climate change (e.g., Sudo et al., 2003; Butchart et al., 2010; Oberländer
473 et al., 2013) in combination with an ozone increase resulting from [modified chemical](#)
474 [production and loss rates in the stratosphere](#)~~stratospheric cooling~~ and enhanced meridional
475 transport (Figure 6f). In contrast, with ODS decrease no significant changes in the downwelling
476 occur (Figure 6h). The small increase in F_{in} (Figure 6g) is therefore attributed to stratospheric
477 ozone recovery from ODS, in particular in Antarctic spring (Figure 6i). Figure 6 also indicates
478 that the maximum change in ~~ozone mass flux~~[OMF](#) into the troposphere occurs at midlatitudes
479 for the GHG increase and at high latitudes for the ODS reduction. This [may have an influence](#)
480 [on can be relevant for](#) the mixing and distribution of stratospheric ozone in the troposphere (see
481 below).

482 Thus, given the positive changes in F_{in} , the significant negative change in the ~~ozone mass~~
483 ~~flux~~[OMF](#) identified in September and October for the ODS decrease, must be attributed to
484 changes in $-dM/dt$ (i.e. the monthly change in the ozone mass contained in the LMS, also
485 referred to as seasonal breathing, [Figure 7](#)). While the total mass in the LMS is decreasing with
486 rising GHG concentrations in the sensitivity simulations (possibly due to the tropopause lifting
487 effect of rising GHGs), it slightly increases with ODS change only (not shown). The mass of
488 ozone (M), however, is increasing globally due to both, GHGs and ODS. Thus, for the GHG
489 effect, the future increase of ozone in the LMS outweighs the reduction in total LMS mass. If
490 this future increase of M in the LMS is monthly varying, a future change (positive or negative)

491 in $-dM/dt$ will result. [This change in \$-dM/dt\$ \(i.e. the seasonal breathing\) is shown in Figure 7.](#)
492 ~~Exactly this is happening in~~ [In](#) SH spring, when the ozone mass increase is steadily amplified
493 between August and November due to the decline of ODS, [a considerable change in \$-dM/dt\$](#)
494 [results](#). This ~~results in~~ [leads to](#) the shift of the seasonality of the ~~ozone mass flux~~ [OMF](#) and
495 therefore to negative changes in SH spring. ~~Der~~

496 As mentioned above, the timing of the strongest input of stratospheric ozone into the
497 troposphere is relevant in that the efficiency of mixing down to lower altitudes or to the surface
498 depends on the chemical lifetime of ozone which varies with season. A shift of the spring
499 maximum in the SH to summer ([December/January](#)) for instance may result in different mean
500 abundances of O₃s in the troposphere. Furthermore, the chemical loss of ozone will increase in
501 a warmer troposphere, affecting the lifetime of ozone and thus the distribution of stratospheric
502 ozone in the troposphere.

503 The future changes in the distribution of O₃s mixing ratios are shown in Figure [87](#) for June.
504 O₃s is projected to increase throughout the extra-tropical troposphere. The largest changes will
505 occur in the subtropics in the upper and middle troposphere, the regions where cross-tropopause
506 transport along isentropic surfaces is possible and ozone is efficiently transported into the
507 troposphere through tropopause folds. This pattern is caused by the rising GHG concentrations
508 (Figure [87b](#)). Near the surface however, the O₃s mixing ratios will decrease with GHG change
509 at summer NH mid-latitudes, either induced by an increased chemical O₃s loss or dry
510 deposition. The total positive change near the surface results from the O₃s increase due to ODS
511 change (Figure [87c](#)). In the SH, the abundance of stratospheric ozone increases throughout the
512 troposphere down to the surface. ~~Here, m~~ [More O₃s seems to be transported is present](#) further
513 down than in the NH, which may be related to the longer chemical lifetime of ozone in winter.
514 This is also obvious from the ODS-induced changes, albeit with very small signals.

515 The annual mean column-integrated values of O₃s and ozone in the troposphere and their
516 respective changes are listed in Table 3. The O₃s column increases globally by 42-% between
517 the years 2000 and 2100, with a larger change occurring in the SH than in the NH. Consistent
518 with the results above, the ~~main contribution is from the GHG changes~~ the change due to GHG
519 is larger than due to ODS, ~~whereas the ODS changes have the largest effect on the SH (+6-%).~~
520 As expected the ODS decrease has a larger effect on the SH (+6%) than on the NH (+2%).
521 ~~These changes may result from the combination of an increased/monthly shifted ozone mass~~
522 ~~flux~~OMF into the troposphere, increased chemical loss of O₃s and changes in dry deposition
523 ~~of O₃s.~~ By splitting the increase in the total burden of tropospheric ozone
524 (=O₃s+O₃t) between 2000 and 2100 into the single components O₃s and O₃t (derived from
525 Table 3), ~~indicates we find~~ that the main contribution to the change is from O₃s (19-%), whereas
526 ozone produced in the troposphere (O₃t, calculated as residual) causes an increase of 12-%
527 summing up to a total increase of 31-% of tropospheric ozone. ~~The larger increase in the~~
528 ~~chemical loss of O₃s compared to the increase in the ozone mass flux~~OMF indicates changing
529 ~~chemical conditions in the troposphere due to climate change.~~ The larger increase in the ozone
530 mass flux (Table 2) compared to the increase of O₃s columns in the troposphere indicates
531 changing chemical conditions in the troposphere due to climate change. This means that the
532 larger amount of stratospheric ozone entering the troposphere does not accumulate to the
533 equivalent larger abundance of O₃s in the troposphere.

534 Next we investigate, to what extent the future change in O₃s (Figure 98, middle row)
535 contributes to the ozone change (Figure 98, top row) in the troposphere. The relative
536 contribution is shown in Figure 98 (bottom row) as annual cycle of the tropospheric columns
537 for (c) the change between 2000 and 2100 due to all forcings, (f) the respective change due to
538 GHGs, and (i) the respective change due to ODS. We find that at SH middle and high latitudes
539 more than 80-% of the increase in tropospheric ozone column is caused by ozone originating

540 from the stratosphere from April through October. A similarly strong contribution to the overall
541 change of more than 80% occurs in the NH extratropics, however confined to the spring season
542 (March, April and May). For the rest of the year, ozone originating from the stratosphere causes
543 more than 50% of the total change in both hemispheres. In contrast, in the tropics only 20 to
544 50% of the ozone change are attributable to changes in ozone from the stratosphere throughout
545 the year.

546 In addition, our simulations illustrate that the future enhancement of stratospheric ozone import
547 into the troposphere and the resulting tropospheric ozone change will be dominated by the GHG
548 effect. If only the concentrations of ODS would decline between the years 2000 and 2100, a
549 minor increase in tropospheric ozone burden in the (mainly SH) extratropics would form
550 (Figure 98g), which is almost completely attributable to increased stratospheric ozone entering
551 into the troposphere (Figures 98h, 98i). ~~However, only in the simulation with increased GHG~~
552 ~~concentrations, the patterns and the amount of tropospheric ozone increase (Figure 8d) and the~~
553 ~~contribution of stratospheric ozone to this increase (Figure 8e), as shown in the simulation with~~
554 ~~all forcings (Figures 8a, 8b), are well reproduced. Up~~ In the GHG only simulation up to 80%
555 of the tropospheric ozone trends in SH winter and 70% in NH spring can be explained by
556 increased abundances of ~~stratospheric ozone O₃s due to the GHG effect~~ (Figure 98f). These
557 numbers also indicate the strong increase of tropospheric photochemical ozone production in
558 the future due to the doubling of methane emissions under the RCP8.5 scenario (e.g., Young et
559 al., 2013; Meul et al., 2016). In NH summer, about 50% of the change are due to stratospheric
560 ozone, while in the tropics and the SH summer months, the contribution is less than 40%. ~~This~~
561 ~~reflects the effect of the substantially increased ozone loss rates resulting from the more~~
562 ~~tropical/subtropical downward transport of stratospheric ozone with enhanced GHG~~
563 ~~concentrations. The chemical ozone loss rate in the troposphere in the ODS simulation is less~~
564 ~~influenced and nearly unchanged in the tropics.~~ In summary, Figure 98 shows that as expected

565 the input of stratospheric ozone is the ~~dominant~~ driver of ozone changes in the troposphere, if
566 only ODS levels are reduced. There is no considerable change in tropospheric chemistry due to
567 the larger ODS abundances. In contrast, ~~F~~for the GHG increase we find that other processes,
568 such as tropospheric chemistry, modulate the tropospheric ozone abundance in addition to the
569 increased influx of stratospheric ozone.

570 Finally, we compare the tropospheric O₃s columns derived from the timeslice simulations
571 under the RCP8.5 scenario with the transient simulation using the RCP6.0 scenario. Figure [109a](#)
572 shows the evolution of annual mean tropospheric ozone (solid) and O₃s (dashed) columns for
573 the NH and the SH. Tropospheric ozone increases in the RCP6.0 simulation from 1960 to the
574 middle of the 21st century and slightly declines afterwards in the NH, while it stays nearly
575 constant in the SH. There is very good agreement of the tropospheric ozone column between
576 the transient and timeslice simulations for the year 2000, when both simulations use observed
577 GHG concentrations. Regarding the temporal evolution of O₃s, we find a positive trend in both
578 hemispheres and only a slight decrease in the NH at the end of the 21st century. In the past, an
579 effect of the ODS driven stratospheric ozone loss is overlaid by the GHG related increase in
580 both hemispheres. However, a slightly smaller rise of O₃s in the SH might be an indication.

581 The RCP8.5 scenario (circles) leads to higher values of tropospheric ozone in 2100 which is
582 related to two effects: a larger import of stratospheric ozone and a larger chemical ozone
583 production in the troposphere due to strongly enhanced methane concentrations in the second
584 half of the 21st century in the RCP8.5 scenario (see Meinshausen et al., 2011).

585 The ratio between O₃s and tropospheric ozone (Figure [109b](#)) gives an indication if the role of
586 stratospheric ozone in the troposphere will change in the future. In the past period of the
587 transient simulation (i.e. RCP6.0 scenario), the relative contribution of O₃s decreases from 48
588 % (1960s) to 44-% (1990s) in the NH and from 52-% to 48-% in the SH. This is caused by an

589 increase of ozone produced in the troposphere, which is stronger than the increase of O₃s
590 (Figure 109a). In the future, however, the relative importance of ozone from the stratosphere
591 increases, reaching 49% in the NH and 55% in the SH around the year 2100. Thus, in the
592 RCP6.0 scenario (more than) half of the ozone in the troposphere will originate from the
593 stratosphere in the (SH) NH ~~at~~ by the end of the 21st century.

594 The comparison with the timeslice simulation (RCP8.5 GHG scenario) shows that the
595 abundance contribution of O₃s to O₃ in the troposphere is lower in the year 2000 than in the
596 transient simulation. This is probably caused by the different data sets used for the SST/SIC
597 fields in the timeslice and transient simulation (see Table 1) leading to different tropopause
598 heights and therefore to different tropospheric columns. However, the larger contribution of
599 O₃s to ozone in the SH (48%) compared to the NH (43%) is confirmed. In 2100, tropospheric
600 ozone columns in the NH (SH) will consist ~~of~~ 46% (~~52%~~) of ozone originating from the
601 stratosphere.

602 In summary, in a future RCP6.0 scenario, the relative importance of ozone from the stratosphere
603 in the troposphere will increase by 5% in the NH and 7% in the SH around the year 2100
604 compared to 1990. In the RCP8.5 scenario, the increase will be slightly smaller (3% in the NH
605 and 4% in the SH in 2100 compared to 2000) despite the larger increase in OMF shown in
606 Figure 2. Thus, the increase in the contribution of O₃s in the future is slightly smaller in the
607 RCP8.5 scenario than in the RCP6.0 scenario, despite the larger increase in ozone mass flux
608 shown in Figure 2. Here, the different evolution of tropospheric ozone production in the two
609 GHG scenarios plays a crucial role.

610

611 6. Summary

612 In this study we have analysed the future changes in stratosphere-to-troposphere transport of
613 ozone in timeslice and transient simulations with the CCM EMAC to address the questions
614 brought up in the introduction: (1) How will the stratosphere-to-troposphere ~~ozone-mass~~
615 ~~flux~~OMF change in the future? (2) What are the major drivers of the future changes in
616 stratosphere-to-troposphere ~~ozone-mass flux~~OMF? (3) Will the seasonality of the STE change
617 in future? (4) How will the GHG emission scenarios affect the ~~ozone-mass flux~~OMF into the
618 troposphere? (5) How is the ratio of stratospheric ozone in the troposphere changed in the
619 future?

620 In agreement with other studies (e.g., Sudo et al., 2003; Collins et al., 2003; Hegglin and
621 Shepherd, 2009; Banerjee et al., 2016), we find that the influx of stratospheric ozone into the
622 troposphere will increase in the future. Between 2000 and 2100 the EMAC timeslice
623 simulations project an increase of the annual global mean ~~ozone-mass flux~~OMF by 53-% under
624 the RCP8.5 scenario. Increasing GHG concentrations were identified as the main driver of the
625 rising ~~ozone-mass flux~~OMF into the troposphere by strengthening the BDC and ~~reducing~~
626 ~~chemical ozone loss~~ increasing the net ozone production in a colder the stratosphere. The annual
627 global ~~ozone-mass flux~~OMF is increased by 46-% due to rising GHG concentrations compared
628 to an increase of 7-% due to the ODS decline and the associated ozone recovery. The GHG
629 effect leads to a larger intensification of STE in the NH (51-%) than in the SH (40-%), whereas
630 the ODS effect is most prominent in the SH (9-%) compared to 4-% in the NH.

631 Regarding the seasonal changes of the ~~ozone-mass flux~~OMF, we showed the dominant role of
632 GHG changes for the NH whereas in the SH, both ODS and GHG changes affect the seasonality
633 of the ~~ozone-mass flux~~OMF increase: the GHG increase is the main driver of the increase in
634 winter and spring, but in summer also ODS-induced changes contribute to the ~~ozone-mass~~
635 ~~flux~~OMF increase. Furthermore, the ODS decrease and the concomitant ozone increase in the

636 lower stratosphere during SH spring cause a large change in the seasonal breathing term in the
637 SH from August to October, which results in a shift of the maximum ozone flux to late
638 spring/early summer. The GHG effect leads to a dampened amplitude of the seasonal cycle in
639 the SH and an intensified in the NH. This can have an impact on the distribution of stratospheric
640 ozone in the troposphere: in the SH more ozone is transported into the troposphere in winter,
641 when the chemical lifetimes are relatively long, whereas in the NH the largest increase is found
642 in summer. This may explain the larger increase of O₃s columns in the SH compared to the NH
643 despite the smaller increase in ~~ozone-mass-flux~~OMF (see Table 2 and 3).

644 The future spatial distribution of the tropospheric O₃s column in the troposphere is determined
645 by the change pattern due to GHG increases. Here, the largest increase of O₃s mixing ratios
646 occurs in the subtropical upper troposphere, where stratospheric ozone is transported into the
647 troposphere via tropopause folds and then further down to lower levels in the large-scale sinking
648 of the Hadley cell (Roelofs and Lelieveld, 1997). ODS-related changes in the tropospheric O₃s
649 column are smaller. They show no comparable signal in the subtropical region, but a more
650 homogeneous distribution. In the ODS simulation, the main increase of stratospheric ozone
651 input occurs via the downward branch of the BDC in middle and higher latitudes, where the
652 chemical ozone loss of tropospheric ozone is smaller than in the subtropics and hence mixing
653 towards the surface is more efficient.

654 In the SH winter months, the ozone change due to increased stratospheric ozone influx explains
655 up to 80-% of the overall tropospheric ozone increase under the RCP8.5 scenario by the end of
656 the century. In the rest of the year, the stratospheric ozone changes cover more than 50-% of
657 the ozone changes in the SH troposphere. In contrast, increased stratospheric ozone explains
658 only about 70-% of the ozone changes in NH spring indicating the strong increase of

659 tropospheric photochemical ozone production in the future due to the doubling of methane
660 emissions under the RCP8.5 scenario.

661 The comparison with the transient EMAC simulation under the RCP6.0 scenario shows a
662 smaller future increase in annual global ~~ozone mass flux~~OMF into the troposphere (4.2-%/per
663 decade) than under the RCP8.5 scenario (5.3-%/per decade). In the transient RCP6.0 simulation
664 the positive trend between 2000 and 2100 is larger in the SH than in the NH, which is not found
665 in the RCP8.5 timeslices. The stronger increase in the ~~ozone mass flux~~OMF under the RCP8.5
666 scenario is connected with a larger O₃s column, but the relative contribution of O₃s to ozone
667 in the troposphere rises similarly in both scenarios. This is caused by the different evolution of
668 the ozone produced in the troposphere in the RCP6.0 and RCP8.5 scenario [due to the deviating](#)
669 [emission scenarios for the ozone precursor species](#). In the past, the input of stratospheric ozone
670 has slightly decreased between 1960 and 1999, especially in the SH (-1.4-%/per decade) due
671 to the formation of the ozone hole. However, the O₃s column in the troposphere integrated over
672 the NH and the SH shows a small positive trend. This may be related with the seasonal timing
673 of the changes, since ozone loss in the SH stratosphere has the largest effect on the ~~ozone mass~~
674 ~~flux~~OMF in spring and early summer when the tropospheric ozone loss rates are higher than in
675 winter and mixing is less efficient anyway.

676 In summary, this study shows that GHG and ODS changes have different effects on the future
677 ~~ozone mass flux~~OMF, the seasonality and the resulting abundances of stratospheric ozone in
678 the troposphere. Moreover, it shows that both forcings are projected to cause an increased
679 amount of stratospheric ozone in the troposphere, which will not only contribute to the radiative
680 forcing and global warming but will also affect the air quality at the surface. [Further studies are](#)
681 [needed to investigate and separate the effect of non-methane precursors on the OMF, the](#)
682 [interactions with the increasing GHGs and the resulting distribution of O₃s in the troposphere.](#)

683

684 **Code availability**

685 The Modular Earth Submodel System (MESSy), including the EMAC model, is continuously
686 further developed and applied by a consortium of institutions. The usage of MESSy and access
687 to the source code is licensed to all affiliates of institutions, which are members of the MESSy
688 Consortium. Institutions can become a member of the MESSy Consortium by signing the
689 MESSy Memorandum of Understanding. More information can be found on the MESSy
690 Consortium website (<http://www.messy-interface.org>).

691

692 **Data availability**

693 The data of the ESCiMo simulation RC2-base-05 will be made available in the Climate and
694 Environmental Retrieval and Archive (CERA) database at the German Climate Computing
695 Centre (DKRZ; <http://cera-www.dkrz.de/WDC/wwui/Index.jsp>). The corresponding digital
696 object identifiers (doi) will be published on the MESSy Consortium web page
697 (<http://www.messy-interface.org>). A subset of the RC2-base-05 simulation results has been
698 uploaded to the BADC database for the CCMi project. Data of the EMAC timeslice simulations
699 performed for this for this paper are available at the Freie Universität Berlin on the SHARP
700 data archive under ACPD_ozone_transport_Meul_et_al_2018.tar.

701

702 **Author contribution**

703 SM has performed and analysed the timeslice simulations and has written the manuscript. UL
704 has initialized the study and has considerably contributed to the manuscript and the discussion.

705 PK has contributed to the analysis of the model data. SOH has performed the timeslice
706 simulations and has contributed to the discussion of the results. PJ led the ESCiMo project,
707 coordinated the preparation of the EMAC simulation setups and conducted the model
708 simulations (here RC2-base-05). Moreover, he contributed to the EMAC model development,
709 including the here applied O3s diagnostics.

710

711 **Competing interests**

712 The authors declare that they have no conflict of interest.

713

714 **Special issue statement**

715 This article is part of the special issue “The Modular Earth Submodel System (MESSy)
716 (ACP/GMD inter-journal SI)”. It is not associated with a conference.

717

718 **Acknowledgements**

719 This work has been funded by the Deutsche Forschungsgemeinschaft (DFG) within the DFG
720 Research Unit FOR 1095 “Stratospheric Change and its Role for Climate Prediction” (SHARP)
721 under the grants LA 1025/13-2 and LA 1025/14-2. The authors are grateful to the North-
722 German Supercomputing Alliance (HLRN) for providing computer resources and support. The
723 EMAC model simulation RC2-base-05 was performed at the German Climate Computing
724 Centre (DKRZ) through support from the Bundesministerium für Bildung und Forschung
725 (BMBF). DKRZ and its scientific steering committee are gratefully acknowledged for
726 providing the HPC and data archiving resources for the projects 853 (ESCiMo – Earth System

727 Chemistry integrated Modelling). [The authors wish to thank two anonymous referees for their](#)
728 [helpful comments and Janice Scheffler for supporting the revision.](#)

729

730

731 **References**

732 [Andrews, T., J. M. Gregory, M. J. Webb, and K. E. Taylor \(2012\), Forcing, feedbacks and](#)
733 [climate sensitivity in CMIP5 coupled atmosphere-ocean climate models, *Geophys. Res.*](#)
734 [Lett., 39, L09712, doi:10.1029/2012GL051607.](#)

735 Akritidis, D., Pozzer, A., Zanis, P., Tyrlis, E., Škerlak, B., Sprenger, M., and Lelieveld, J.: On
736 the role of tropopause folds in summertime tropospheric ozone over the eastern
737 Mediterranean and the Middle East, *Atmos. Chem. Phys.*, 16, 14025-14039,
738 doi:10.5194/acp-16-14025-2016, 2016.

739 Appenzeller, C., J. R. Holton, and K. H. Rosenlof: Seasonal variation of mass transport across
740 the tropopause, *J. Geophys. Res.*, 101(D10), 15071-15078, doi:10.1029/96JD00821, 1996.

741 Banerjee, A., Maycock, A. C., Archibald, A. T., Abraham, N. L., Telford, P., Braesicke, P., and
742 Pyle, J. A.: Drivers of changes in stratospheric and tropospheric ozone between year 2000
743 and 2100, *Atmos. Chem. Phys.*, 16, 2727-2746, doi:10.5194/acp-16-2727-2016, 2016.

744 Barré, J., El Amraoui, L., Ricaud, P., Lahoz, W. A., Attié, J.-L., Peuch, V.-H., Josse, B., and
745 Marécal, V.: Diagnosing the transition layer at extratropical latitudes using MLS O3 and
746 MOPITT CO analyses, *Atmos. Chem. Phys.*, 13, 7225-7240, doi:10.5194/acp-13-7225-
747 2013, 2013.

748 Butchart, N., I. Cionni, V. Eyring, T. G. Shepherd, D. W. Waugh, H. Akiyoshi, J. Austin, C.
749 Brühl, M. P. Chipperfield, E. Cordero, M. Dameris, R. Deckert, S. Dhomse, S. M. Frith, R.
750 R. Garcia, A. Gettelman, M. A. Giorgetta, D. E. Kinnison, F. Li, E. Mancini, C. McLandress,

751 S. Pawson, G. Pitari, D. A. Plummer, E. Rozanov, F. Sassi, J.F. Scinocca, K. Shibata, B.
752 Steil, and W. Tian: Chemistry-Climate Model Simulations of Twenty-First Century
753 Stratospheric Climate and Circulation Changes, *J. Clim.*, 23, 5349-5374, 2010.

754 Butchart. N. and Scaife. A.: Removal of chlorofluorocarbons by increased mass exchange
755 between the stratosphere and troposphere in a changing climate, *Nature*, 410, 799-801,
756 doi:10.1038/35071047, 2010.

757 ~~Collins, W. J., R. G. Derwent, C. E. Johnson, and D. S. Stevenson: The impact of human~~
758 ~~activities on the photochemical production and destruction of tropospheric ozone, Q. J. R.~~
759 ~~Meteorol. Soc., 126, 1925-1951, 2000.~~

760 Collins, W. J., R. G. Derwent, B. Garnier, C. E. Johnson, M. G. Sanderson, and D. S. Stevenson:
761 Effect of stratosphere-troposphere exchange on the future tropospheric ozone trend, *J.*
762 *Geophys. Res.*, 108(D12), 8528, doi:10.1029/2002JD002617, 2003.

763 Collins, W. J., Bellouin, N., Doutriaux-Boucher, M., Gedney, N., Halloran, P., Hinton, T.,
764 Hughes, J., Jones, C. D., Joshi, M., Liddicoat, S., Martin, G., O'Connor, F., Rae, J., Senior,
765 C., Sitch, S., Totterdell, I., Wiltshire, A., and Woodward, S.: Development and evaluation
766 of an Earth-System model – HadGEM2, *Geosci. Model Dev.*, 4, 1051–1075,
767 doi:10.5194/gmd-4-1051-2011, 2011.

768 Fischer, H., Wienhold, F. G., Hoor, P., Bujok, O., Schiller, C., Siegmund, P., Ambaum, M.,
769 Scheeren, H. A. and Lelieveld, J.: Tracer correlations in the northern high latitude lowermost
770 stratosphere: Influence of cross-tropopause mass exchange, *Geophysical Research Letters*,
771 27, 1, 97-100, DOI = 10.1029/1999GL010879, 2000.

772 Giorgetta, M. A. and Bengtsson, L.: Potential role of the quasi-biennial oscillation in the
773 stratosphere-troposphere exchange as found in water vapor in general circulation model
774 experiments, *J. Geophys. Res.-Atmos.*, 104, 6003–6019, doi:10.1029/1998JD200112, 1999.

775 Giorgetta, M. A., et al.: Climate and carbon cycle changes from 1850 to 2100 in MPI-ESM
776 simulations for the Coupled Model Intercomparison Project phase 5, *J. Adv. Model. Earth*
777 *Syst.*, 5, 572–597, doi:10.1002/jame.20038, 2013.

778 Hegglin, M. I., and T. G. Shepherd: O₃-N₂O correlations from the Atmospheric Chemistry
779 Experiment: Revisiting a diagnostic of transport and chemistry in the stratosphere, *J.*
780 *Geophys. Res.*, 112, D19301, doi:10.1029/2006JD008281, 2007.

781 Hegglin, M. and T. Shepherd: Large climate-induced changes in ultraviolet index and
782 stratosphere-to-troposphere ozone flux, *Nature Geosci.*, 2, 687 – 691,
783 DOI:10.1038/ngeo604, 2009.

784 [Hegglin, M. I., C. D. Boone, G. L. Manney, K. A. Walker, A global view of the extratropical](#)
785 [tropopause transition layer from Atmospheric Chemistry Experiment Fourier Transform](#)
786 [Spectrometer O₃, H₂O, and CO, *J. Geophys. Res.*, 114, D00B11,](#)
787 [doi:10.1029/2008JD009984, 2009.](#)

788 Holton, J. R., P. H. Haynes, M. E. McIntyre, A. R. Douglass, R. B. Rood, and L. Pfister:
789 Stratosphere-troposphere exchange, *Rev. Geophys.*, 33(4), 403–439, 1995.

790 Intergovernmental Panel on Climate Change: Climate change 2001: The scientific basis,
791 Contribution of Working Group 1 to the Third Assessment Report, Cambridge, United
792 Kingdom and New York, NY, USA, 2001.

793 Jöckel, P., Tost, H., Pozzer, A., Brühl, C., Buchholz, J., Ganzeveld, L., Hoor, P., Kerkweg, A.,
794 Lawrence, M. G., Sander, R., Steil, B., Stiller, G., Tanarhte, M., Taraborrelli, D., van
795 Aardenne, J., & Lelieveld, J.: The atmospheric chemistry general circulation model
796 ECHAM5/MESSy1: consistent simulation of ozone from the surface to the mesosphere,
797 *Atmospheric Chemistry and Physics*, 6, 5067–5104, doi: 10.5194/acp-6-5067-2006, URL
798 <http://www.atmos-chem-phys.net/6/5067/2006/>, 2006.

799 Jöckel, P., Tost, H., Pozzer, A., Kunze, M., Kirner, O., Brenninkmeijer, C. A. M., Brinkop, S.,
800 Cai, D. S., Dyroff, C., Eckstein, J., Frank, F., Garny, H., Gottschaldt, K.-D., Graf, P., Grewe,
801 V., Kerkweg, A., Kern, B., Matthes, S., Mertens, M., Meul, S., Neumaier, M., Nützel, M.,
802 Oberländer-Hayn, S., Ruhnke, R., Runde, T., Sander, R., Scharffe, D., and Zahn, A.: Earth
803 System Chemistry integrated Modelling (ESCiMo) with the Modular Earth Submodel
804 System (MESSy) version 2.51, *Geosci. Model Dev.*, 9, 1153-1200, doi:10.5194/gmd-9-
805 1153-2016, 2016.

806 Johnson, C. E., Collins, W. J., Stevenson, D. S., and Derwent, R. G.: Relative roles of climate
807 and emissions changes on future tropospheric oxidant concentrations, *J. Geophys. Res.-*
808 *Atmos.*, 104, 18631–18645, doi:10.1029/1999JD900204, 1999.

809 Jonsson, A. I., J. de Grandpré, V. I. Fomichev, J. C. McConnell and S. R. Beagley: Doubled
810 CO₂-induced cooling in the middle atmosphere: Photochemical analysis of the ozone
811 radiative feedback, *J. Geophys. Res.*, 109, D24103, doi:10.1029/2004JD005093, 2004.

812 (The HadGEM2 Development Team): Martin, G. M., Bellouin, N., Collins, W. J., Culverwell,
813 I. D., Halloran, P. R., Hardiman, S. C., Hinton, T. J., Jones, C. D., McDonald, R. E.,
814 McLaren, A. J., O'Connor, F. M., Roberts, M. J., Rodriguez, J. M., Woodward, S., Best, M.
815 J., Brooks, M. E., Brown, A. R., Butchart, N., Dearden, C., Derbyshire, S. H., Dharssi, I.,
816 Doutriaux-Boucher, M., Edwards, J. M., Falloon, P. D., Gedney, N., Gray, L. J., Hewitt, H.
817 T., Hobson, M., Huddleston, M. R., Hughes, J., Ineson, S., Ingram, W. J., James, P. M.,
818 Johns, T. C., Johnson, C. E., Jones, A., Jones, C. P., Joshi, M. M., Keen, A. B., Liddicoat,
819 S., Lock, A. P., Maidens, A. V., Manners, J. C., Milton, S. F., Rae, J. G. L., Ridley, J. K.,
820 Sellar, A., Senior, C. A., Totterdell, I. J., Verhoef, A., Vidale, P. L., and Wiltshire, A.: The
821 HadGEM2 family of Met Office Unified Model climate configurations, *Geosci. Model Dev.*,
822 4, 723–757, doi:10.5194/gmd-4-723-2011, 2011.

823 Meinshausen, M., S. J. Smith, K. V. Calvin, J. S. Daniel, M. L. T. Kainuma, J.-F. Lamarque,
824 K. Matsumoto, S. A. Montzka, S. C. B. Raper, K. Riahi, A. M. Thomson, G. J. M. Velders
825 and D. van Vuuren: The RCP Greenhouse Gas Concentrations and their Extension from
826 1765 to 2300, *Climatic Change (Special Issue)*, doi: 10.1007/s10584-011-0156-z, 2011.
827

828 Meul, S., M. Dameris, U. Langematz, J. Abalichin, A. Kerschbaumer, A. Kubin, and S.
829 Oberländer-Hayn: Impact of rising greenhouse gas concentrations on future tropical ozone
830 and UV exposure, *Geophys. Res. Lett.*, 43, 2919–2927, doi:10.1002/2016GL067997, 2016.
831 [Meul, S., U. Langematz, S. Oberländer, H. Garny, and P. Jöckel: Chemical contribution to](#)
832 [future tropical ozone change in the lower stratosphere, *Atmos. Chem. Phys.*, 14, 2959–2971,](#)
833 [doi:10.5194/acp-14-2959-2014, 2014.](#)

834 [Monks, P. S., et al.: Atmospheric composition change – global and regional air quality,](#)
835 [Atmospheric Environment, 43, 33, 5268–5350, doi:10.1016/j.atmosenv.2009.08.021, 2009.](#)

836 Neu, J. L., T. Flury, G. L. Manney, M. L. Santee, N. J. Livesey, and J. Worden: Tropospheric
837 ozone variations governed by changes in stratospheric circulation, *Nat. Geosci.*, 7(5), 340-
838 344, doi:10.1038/ngeo2138, 2014.

839 [Nevison, C. D., S. Solomon, and R. S. Gao: Buffering interactions in the modeled response of](#)
840 [stratospheric O₃ to increased NO_x and HO_x, *J. Geophys. Res.*, 104\(D3\), 3741–3754,](#)
841 [doi:10.1029/1998JD100018, 1999.-](#)

842 Oberländer, S., U. Langematz, and S. Meul: Unraveling impact factors for future changes in
843 the Brewer-Dobson circulation, *J. Geophys. Res. Atmos.*, 118, doi: 10.1002/jgrd.50775,
844 2013.

845 [Olsen, S. C., McLinden, C. A., and Prather, M. J.: Stratospheric N₂O–NO_y system: Testing](#)
846 [uncertainties in a three-dimensional framework, *J. Geophys. Res.*, 106, 28771,](#)
847 [doi:10.1029/2001JD000559, 2001.](#)

848 ~~Olsen, M. A., A. R. Douglass, and M. R. Schoeberl: Estimating downward cross-tropopause~~
849 ~~ozone flux using column ozone and potential vorticity, *J. Geophys. Res.*, 107(D22), 4636,~~
850 ~~doi:10.1029/2001JD002041, 2002.~~

851 Ordóñez, C., D. Brunner, J. Staehelin, P. Hadjinicolaou, J. A. Pyle, M. Jonas, H. Wernli, and
852 A. S. H. Prévôt: Strong influence of lowermost stratospheric ozone on lower tropospheric
853 background ozone changes over Europe, *Geophys. Res. Lett.*, 34, L07805,
854 doi:10.1029/2006GL029113, 2007.

855 [Pan, L. L., J. C. Wei, D. E. Kinnison, R. R. Garcia, D. J. Wuebbles, and G. P. Brasseur: A set](#)
856 [of diagnostics for evaluating chemistry-climate models in the extratropical tropopause](#)
857 [region, *J. Geophys. Res.*, 112, D09316, doi:10.1029/2006JD007792, 2007.](#)

858 [Revell, L. E., Bodeker, G. E., Huck, P. E., Williamson, B. E., and Rozanov, E.: The sensitivity](#)
859 [of stratospheric ozone changes through the 21st century to N₂O and CH₄, *Atmos. Chem.*](#)
860 [Phys., 12, 11309-11317, https://doi.org/10.5194/acp-12-11309-2012, 2012.](#)

861 Roelofs, G.-J. and Lelieveld, J.: Model study of the influence of cross-tropopause O₃ transports
862 on tropospheric O₃ levels, *Tellus B*, 49, 38–55, 1997.

863 Sander, R., Baumgaertner, A., Gromov, S., Harder, H., Jöckel, P., Kerkweg, A., Kubistin, D.,
864 Regelin, E., Riede, H., Sandu, A., Taraborrelli, D., Tost, H., and Xie, Z.-Q.: The atmospheric
865 chemistry box model CAABA/MECCA-3.0, *Geosci. Model Dev.*, 4, 373–380,
866 doi:10.5194/gmd-4-373-2011, 2011a.

867 Sander, S. P., Abbatt, J., Barker, J. R., Burkholder, J. B., Friedl, R. R., Golden, D. M., Huie, R.
868 E., Kolb, C. E., Kurylo, M. J., Moortgat, G. K., Orkin, V. L., and Wine, P. H.: Chemical
869 Kinetics and Photochemical Data for Use in Atmospheric Studies, Evaluation No. 17, JPL
870 Publication 10-6, Jet Propulsion Laboratory, Pasadena, available at:
871 <http://jpldataeval.jpl.nasa.gov> (last access: 23 March 2016), 2011b.

872 Shindell, D. T., et al.: Simulations of preindustrial, present-day, and 2100 conditions in the
873 NASA GISS composition and climate model G-PUCCINI, *Atmos. Chem. Phys.*, 6, 4427–
874 4459, 2006.

875 Schmidt, H., S. Rast, F. Bunzel, M. Esch, M. Giorgetta, S. Kinne, T. Krismer, G. Stenchikov,
876 C. Timmreck, L. Tomassini, and M. Walz: Response of the middle atmosphere to
877 anthropogenic and natural forcings in the CMIP5 simulations with the Max Planck Institute
878 Earth system model, *J. Adv. Model. Earth Syst.*, 5, 98–116, doi:10.1002/jame.20014, 2013.

879 Škerlak, B., Sprenger, M., and Wernli, H.: A global climatology of stratosphere-troposphere
880 exchange using the ERA-Interim data set from 1979 to 2011, *Atmos. Chem. Phys.*, 14, 913-
881 937, doi:10.5194/acp-14-913-2014, 2014.

882 [Stevenson, D. S., Dentener, F. J., Schultz, M. G., Ellingsen, K., van Noije, T. P. C., Wild, O.,](#)
883 [Zeng, G. Amann, M., Atherton, C. S., Bell, N., Bergmann, D. J., Bey, I., Butler, T., Cofala,](#)
884 [J., Collins, W. J., Derwent, R. G., Doherty, R. M., Drevet, J., Eskes, H. J., Fiore, A. M.,](#)
885 [Gauss, M., Hauglustaine, D. A., Horowitz, L. W., Isaksen, I. S. A., Krol, M. C., Lamarque,](#)
886 [J.-F., Lawrence, M. G., Montanaro, V., Müller, J.-F., Pitari, G., Prather, M. J., Pyle, J. A.,](#)
887 [Rast, S., Rodriguez, J. M., Sanderson, M. G., Savage, N. H., Shindell, D. T., Strahan, S. E.,](#)
888 [Sudo, K., and Szopa, S.: Multimodel ensemble simulations of present-day and near-future](#)
889 [tropospheric ozone, *J. Geophys. Res.*, 111, D08301, doi:10.1029/2005JD006338, 2006.](#)

890 Stohl, A., et al.: Stratosphere-troposphere exchange: A review, and what we have learned from
891 STACCATO, *J. Geophys. Res.*, 108 (D12), 8516, doi:10.1029/2002JD002490, 2003.

892 Sudo, K., M. Takahashi, and H. Akimoto: Future changes in stratosphere-troposphere exchange
893 and their impacts on future tropospheric ozone simulations, *Geophys. Res. Lett.*, 30(24),
894 2256, doi:10.1029/2003GL018526, 2003.

895 Tian, W., M. P. Chipperfield, D. S. Stevenson, R. Damoah, S. Dhomse, A. Dudhia, H.
896 Pumphrey, and P. Bernath: Effects of stratosphere-troposphere chemistry coupling on
897 tropospheric ozone, *J. Geophys. Res.*, 115, D00M04, doi:10.1029/2009JD013515, 2010.

898 [Wild, O.: Modelling the global tropospheric ozone budget: exploring the variability in current](#)
899 [models, *Atmos. Chem. Phys.*, 7, 2643–2660, doi:10.5194/acp-7-2643-2007, 2007.](#)

900 WMO (World Meteorological Organisation): Scientific Assessment of Ozone Depletion: 2010,
901 Global Ozone Research and Monitoring Project-Report No. 52, 516 pp., World Meteorol.
902 Organ., Geneva, Switzerland, 2011.

903 WMO (World Meteorological Organisation): Scientific Assessment of Ozone Depletion: 2014,
904 Global Ozone Research and Monitoring Project-Report No. 55, 416 pp., World Meteorol.
905 Organ., Geneva, Switzerland, 2014.

906 Young, P. J., Archibald, A. T., Bowman, K. W., Lamarque, J.-F., Naik, V., Stevenson, D. S.,
907 Tilmes, S., Voulgarakis, A., Wild, O., Bergmann, D., Cameron-Smith, P., Cionni, I., Collins,
908 W. J., Dalsøren, S. B., Doherty, R. M., Eyring, V., Faluvegi, G., Horowitz, L. W., Josse, B.,
909 Lee, Y. H., MacKenzie, I. A., Nagashima, T., Plummer, D. A., Righi, M., Rumbold, S. T.,
910 Skeie, R. B., Shindell, D. T., Strode, S. A., Sudo, K., Szopa, S., and Zeng, G.: Pre-industrial
911 to end 21st century projections of tropospheric ozone from the Atmospheric Chemistry and
912 Climate Model Intercomparison Project (ACCMIP), *Atmos. Chem. Phys.*, 13, 2063-2090,
913 doi:10.5194/acp-13-2063-2013, 2013.

914 Zeng, G., and J. A. Pyle: Changes in tropospheric ozone between 2000 and 2100 modeled in a
915 chemistry-climate model, *Geophys. Res. Lett.*, 30(7), 1392, doi:10.1029/2002GL016708,
916 2003.

917 Zeng, G., O. Morgenstern, P. Braesicke, and J. A. Pyle: Impact of stratospheric ozone recovery
918 on tropospheric ozone and its budget, *Geophys. Res. Lett.*, 37, L09805,
919 doi:10.1029/2010GL042812, 2010.

920 **Table 1.** EMAC CCM simulations used in this study.

| Name | Run mode | GHG (CO₂ , CH₄ , N₂O) | Tropos. O3 precursor (CO , NO_x , NMVOCs) | ODS | SST/SIC |
|--|---|--|--|--------------------------|----------------------|
| RCP6.0 (referred to as RC2-base-05 in Jöckel et al., 2016) | Transient (1960-2099, after 10 years spinup) | RCP6.0 | RCP6.0 | Observations and A1 | HadGEM 1960-2099 |
| REF2000 | Timeslice (40 years, after 5 years spinup) | Observations for 2000 | Observations for 2000 | Observations for 2000 | MPI-ESM 1995-2004 |
| REF2100 | Timeslice (40 years, after 5 years spinup) | RCP8.5 for 2100 | RCP8.5 for 2100 | A1 for 2100 | MPI-ESM 2095-2104 |
| GHG2100 | Timeslice (40 years, after 5 years spinup) | RCP8.5 for 2100 | Observations for 2000 | Obs. for 2000 | MPI-ESM 2095-2104 |
| ODS2100 | Timeslice (40 years, after 5 years spinup) | Observations for 2000 | Observations for 2000 | A1 for 2100 | MPI-ESM 1995-2004 |

921 **Table 2.** Overview of the annual ozone mass flux into the troposphere and the corresponding
 922 standard deviations in the EMAC timeslice simulations. Gray numbers indicate the change
 923 relative to the REF2000 simulation. [All changes are significant on the 95% confidence level.](#)

| | O3 mass flux [Tg/yr] | | |
|---------|-------------------------|-----------------------|-----------------------|
| | global mean | NH | SH |
| REF2000 | 712±26 | 390±18 | 322±16 |
| REF2100 | 1088±43 +53% | 598±29 +53% | 490±23 +52% |
| GHG2100 | 1041± 36 +46% | 590±28 +51% | 451±26 +40% |
| ODS2100 | 758±26 +7% | 406±20 +4% | 352±13 +9% |

924

925

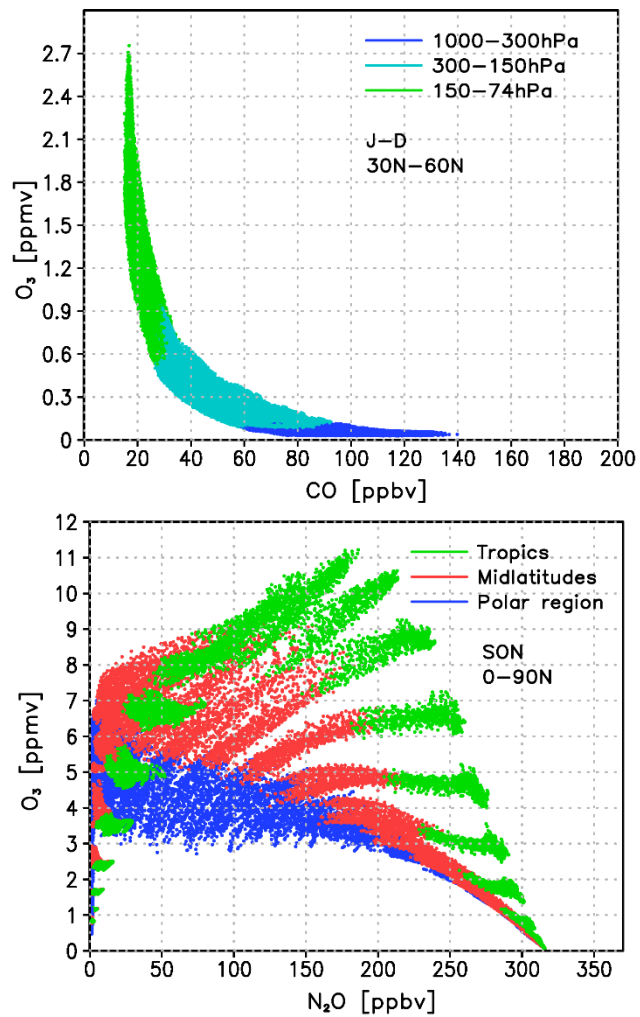
926 **Table 3.** Overview of the annual mean tropospheric O₃ and O₃s burden [Tg] [in the troposphere](#)
 927 with the corresponding standard deviations in the EMAC timeslice simulations. Grey numbers
 928 indicate the change relative to the REF2000 simulation. [All changes are significant on the 95%](#)
 929 [confidence level.](#)

930

| | Tropospheric O ₃ column [Tg] | | | Tropospheric O ₃ s column [Tg] | | |
|---------|---|-----------------------|----------------------|---|-----------------------|-----------------------|
| | global mean | NH | SH | global mean | NH | SH |
| REF2000 | 401±2 | 222±2 | 179±1 | 182 ±3 | 96 ±2 | 86 ±2 |
| REF2100 | 527±3 +31% | 290±2 +31% | 237±2 +32% | 258 ±4 +42% | 134 ±2 +40% | 123 ±2 +43% |
| GHG2100 | 513±3 +28% | 282± 2 +27% | 231±2 +29% | 246 ±3 +35% | 128 ±2 +33% | 118 ±2 +37% |
| ODS2100 | 409±2 +2% | 225±2 +1% | 184±1 +3% | 189 ±2 +4% | 98 ±1 2% | 91 ±1 +6% |

931

932
933
934
935
936
937
938
939
940
941
942
943
944
945
946
947
948
949



950 **Figure 1:** Top: O₃-CO scatter plot for the months January to December in the latitude band
951 30°-60°N for the REF2000 simulation from the troposphere to the lower stratosphere. Color
952 coding indicates different height regions. Bottom: O₃-N₂O scatter plot for the months
953 September to November in the nNorthern hHemisphere for the REF2000 simulation for the
954 altitude region between 270 and 0.1 hPa. Color coding indicates different latitude bands.

955
 956
 957
 958
 959
 960
 961
 962
 963
 964
 965
 966
 967
 968
 969
 970
 971
 972
 973
 974
 975
 976
 977
 978
 979
 980

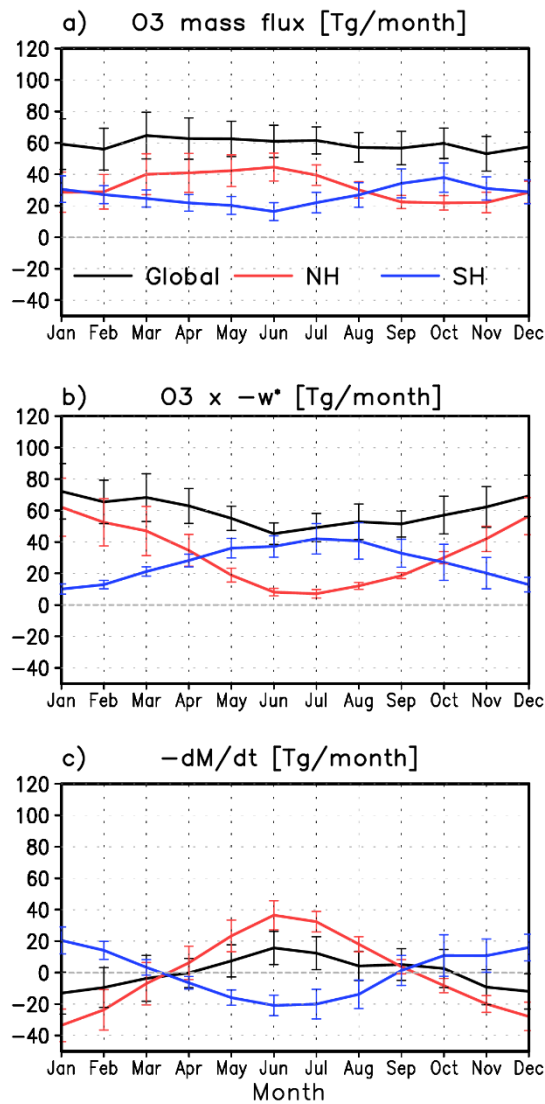


Figure 2: a) Annual ozone mass flux and its 95% confidence interval (i.e. $\pm 2\sigma$, with σ := standard deviation) [Tg/month] from the stratosphere into the troposphere (F_{out}) in the REF2000 simulation integrated globally (black), over the northern (red) and southern (blue) hemispheres. b) As a) but for F_{in} (the product between the ozone concentration and the negative zonal mean residual vertical velocity \bar{w}^* at 91 hPa). c) As a) but for the negative monthly change in ozone mass of the LMS ($-dM/dt$), also referred to as seasonal breathing.

981
982
983
984
985
986
987
988
989
990
991
992
993
994
995
996
997
998
999
1000
1001
1002
1003
1004
1005
1006

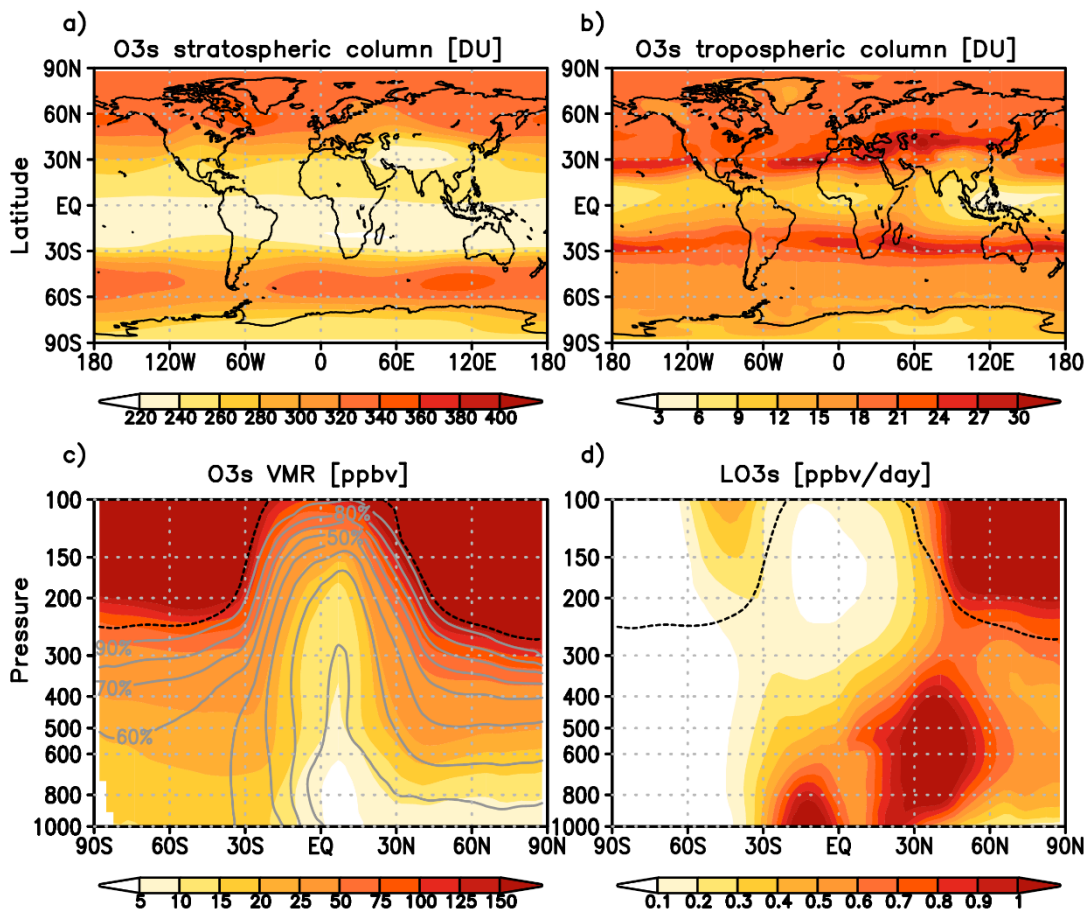
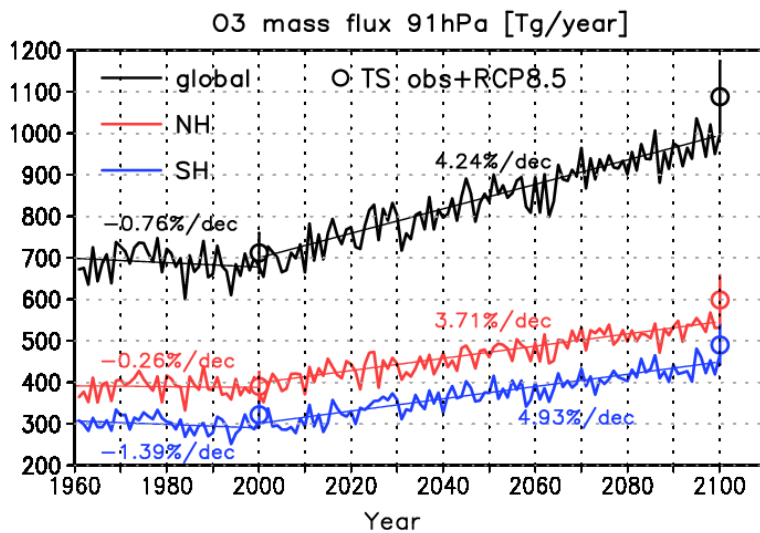


Figure 3: a) Geographical distribution of stratospheric partial columns of the diagnostic O3s tracer in Dobson Units (DU) in June for the REF2000 simulation. b) as a) but for the tropospheric columns. c) Latitude-height section of the O3s volume mixing ratios [ppbv] and d) latitude-height section of the chemical loss rate of O3s [ppbv/day]. The black dashed line indicates the position of the mean tropopause. Gray contour lines in c) show the relative contribution of O3s to the ozone field in %.

1007

1008

1009



1010

1011

1012 **Figure 4:** Temporal evolution of the ozone mass flux [Tg/year] into the troposphere from 1960
1013 to 2099 in the transient RCP6.0 simulation integrated globally (black), over the northern (red),
1014 and southern (blue) hemispheres. The thin lines indicate the linear fits for the sub-periods 1960
1015 to 2000 and 2000 to 2099. In addition, the ozone mass fluxes derived from the timeslice
1016 simulations (TS) for the years 2000 (REF2000) and 2100 (REF2100, RCP8.5 scenario) are
1017 shown by open circles including the $\pm 2\sigma$ range.

1018

1019
 1020
 1021
 1022
 1023
 1024
 1025
 1026
 1027
 1028
 1029
 1030
 1031
 1032
 1033
 1034
 1035
 1036
 1037
 1038
 1039
 1040
 1041
 1042
 1043
 1044

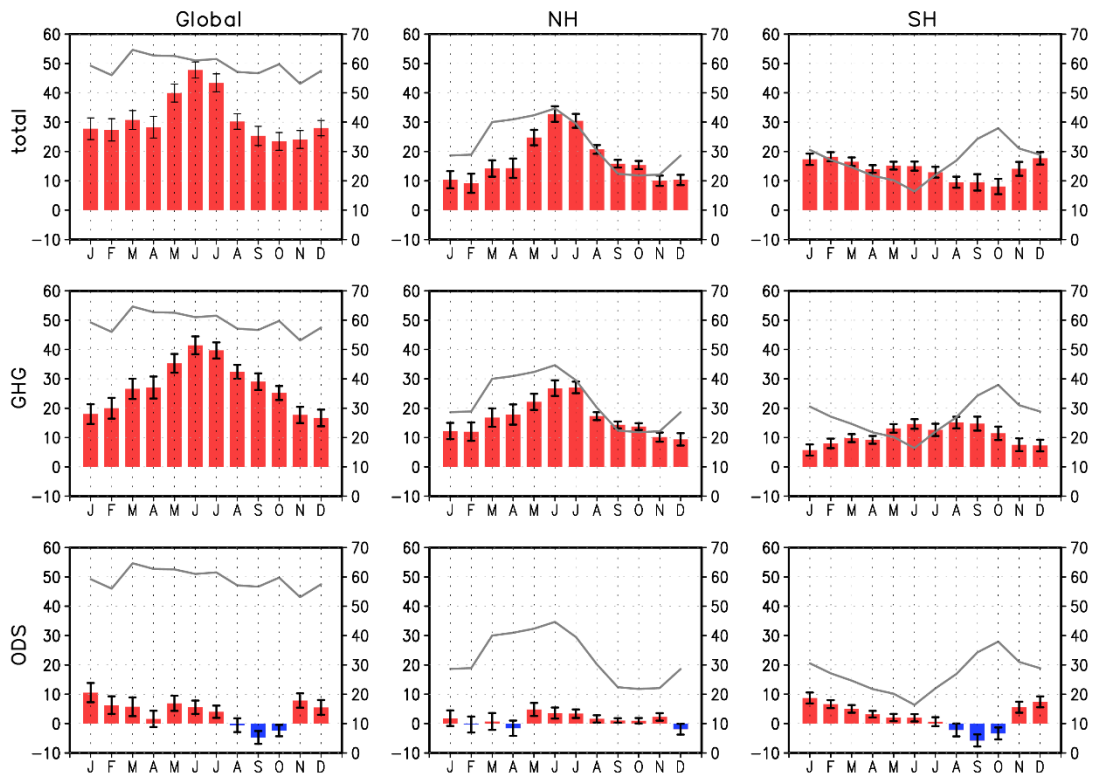
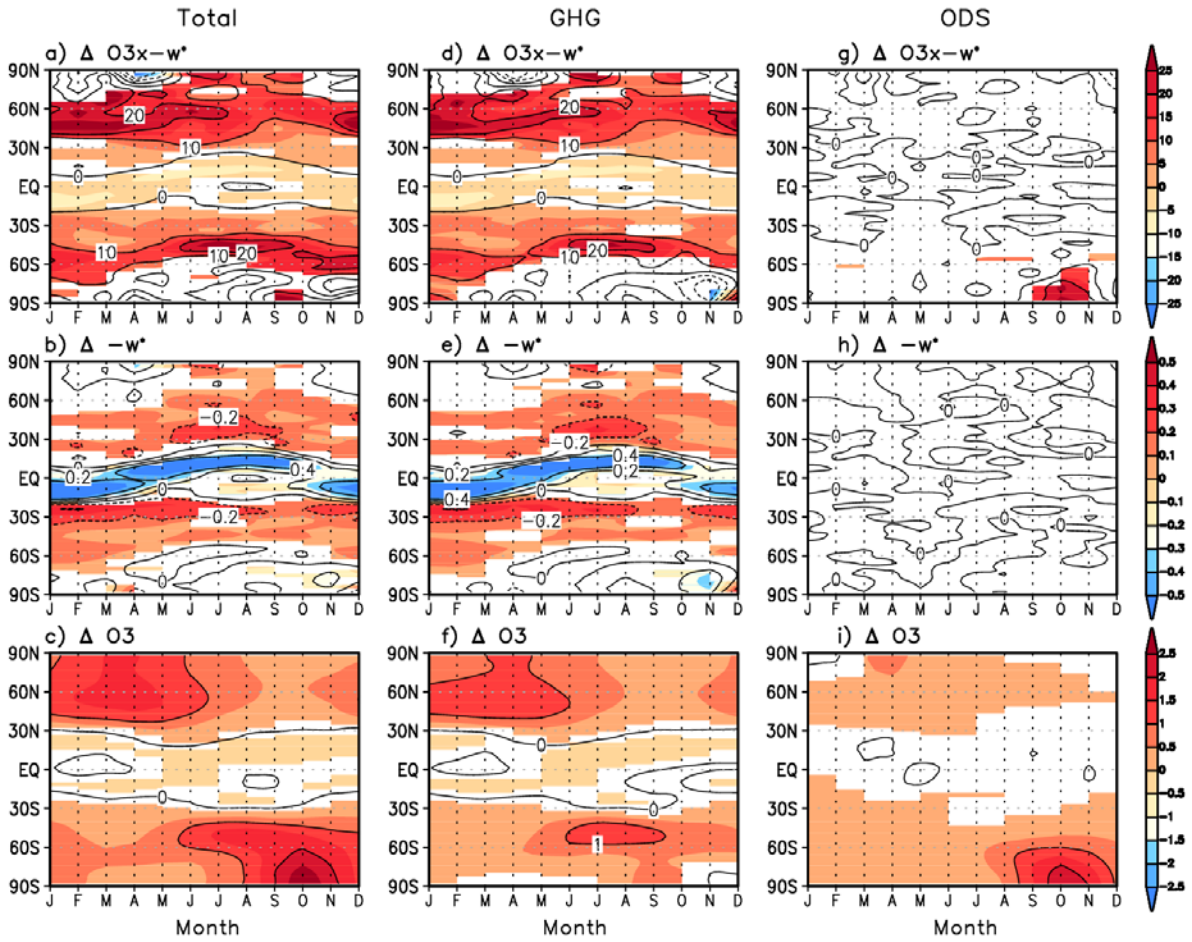


Figure 5: Annual cycle of ozone mass flux changes between 2000 and 2100 [Tg/month] in the timeslice simulations integrated globally (left), over the NH (middle), and over the SH (right) for the changes due to all forcings ~~between 2000 and 2100~~ (top row), the effect of increasing GHG concentrations (middle row) and the impact of declining ODS levels (bottom row). The black error bars denote the $\pm 2\sigma$ standard deviation. The absolute ozone mass flux of the reference simulation REF2000 is shown as grey line with the corresponding y-axis on the right.

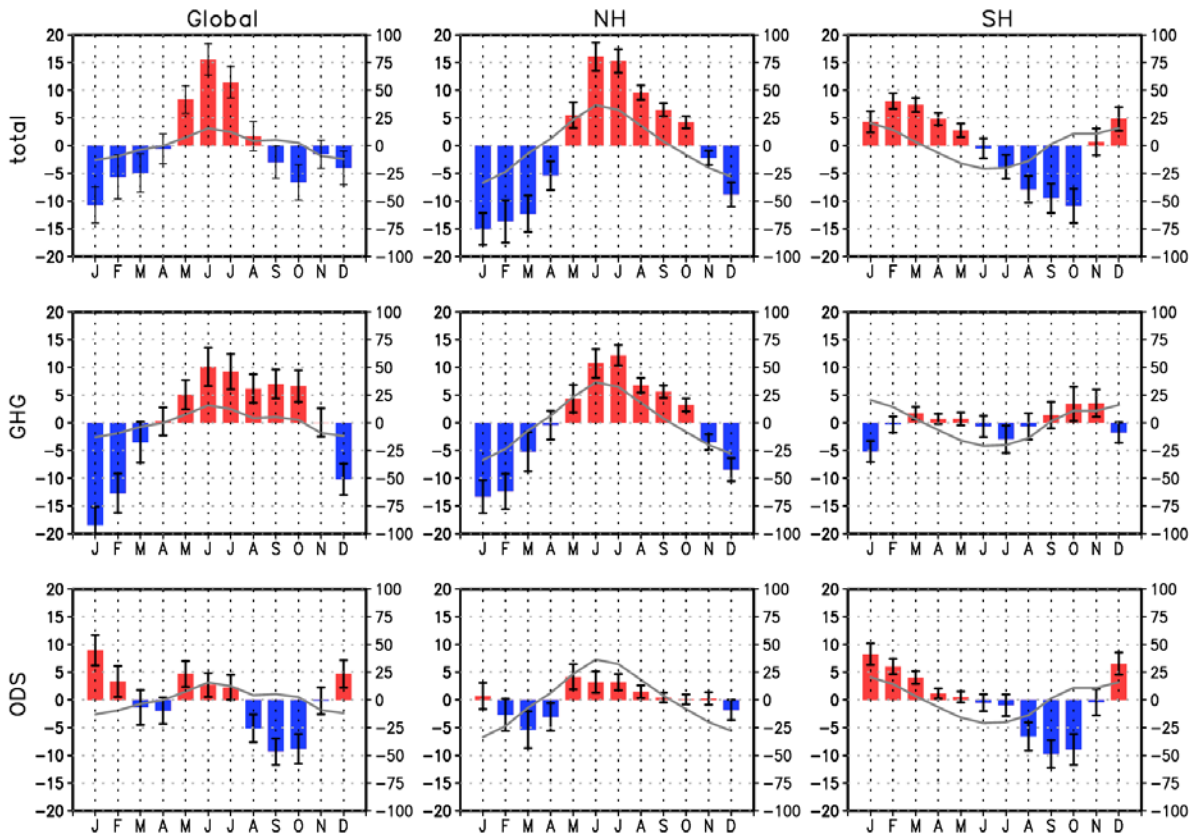


1045

1046

1047 **Figure 6:** Annual cycle of the zonal mean change at 91 hPa in the timeslice simulations due to
 1048 all forcings between 2000 and 2100 (left column), due to GHG increase (middle column), and
 1049 due to ODS decrease (right column). Upper row: changes in the product of ozone concentration
 1050 and $-\bar{w}^*$ [$10^6 \text{ g/cm}^2/\text{month}$], which equals F_{in} when integrated over all latitudes. Middle row:
 1051 changes in $-\bar{w}^*$ [mm/s]. Bottom row: changes in the ozone concentration [molecules/cm²].
 1052 Significant changes on the 95-% confidence level are colored.

1053



1055

1056

1057 **Figure 7:** As Figure 5 but for the change in seasonal breathing ($-dM/dt$) [Tg/month]. The
1058 absolute value for $-dM/dt$ of the reference simulation REF2000 is shown as grey line with the
1059 corresponding y-axis on the right.

1060

1061
1062
1063
1064
1065
1066
1067
1068
1069
1070
1071
1072
1073
1074
1075
1076
1077
1078
1079
1080
1081
1082
1083
1084
1085
1086

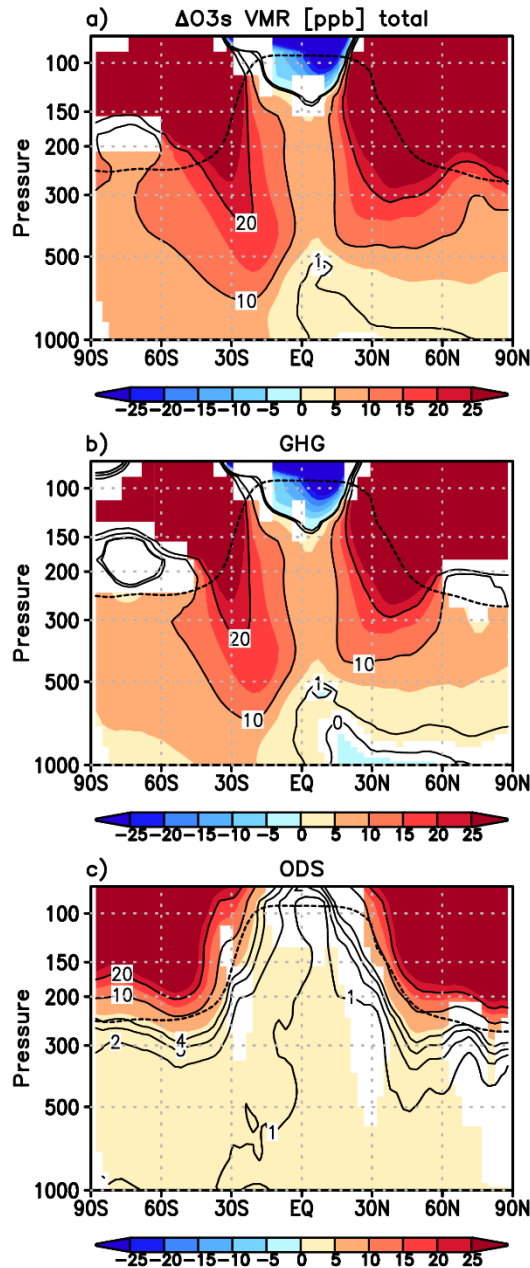
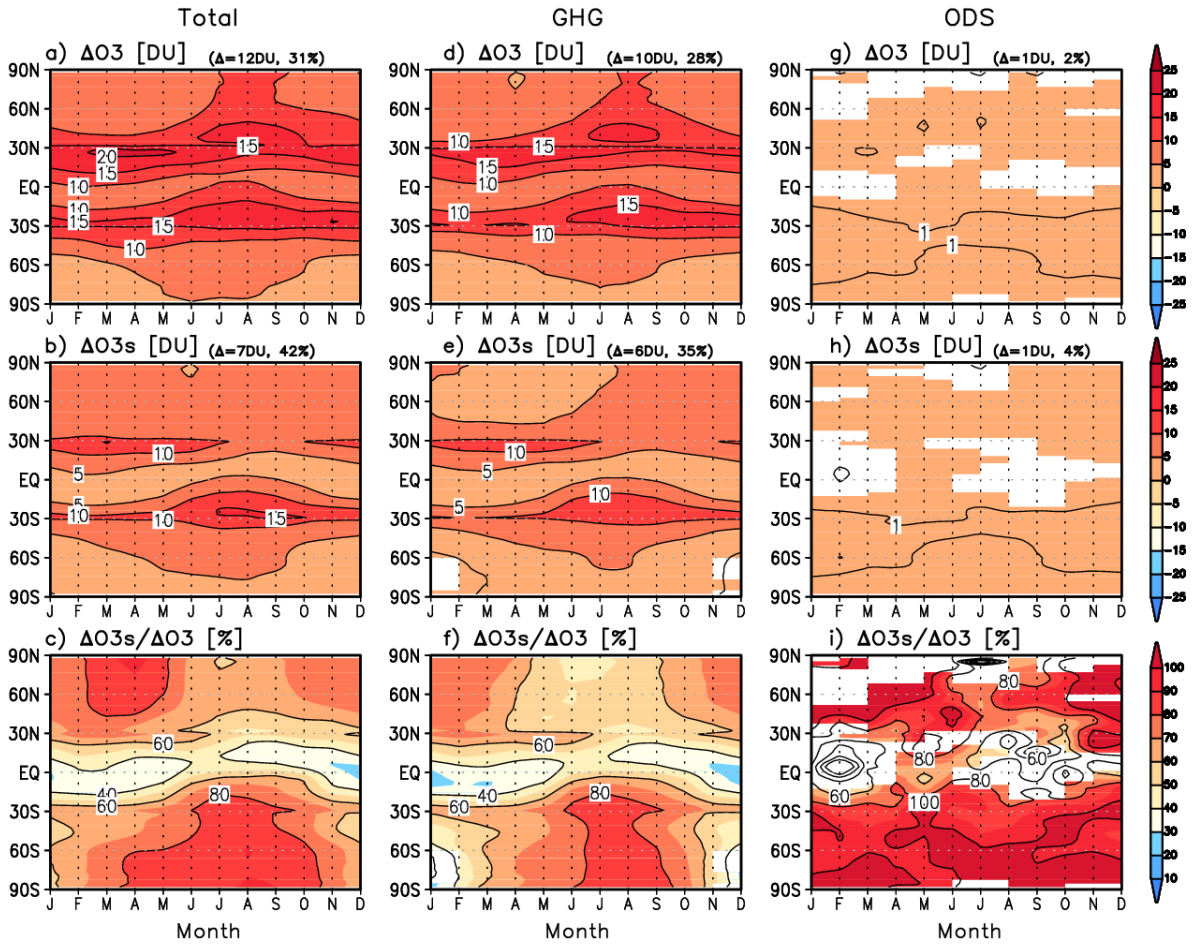


Figure 87: Changes in the volume mixing ratios [ppbv] of the diagnostic tracer O₃s for a) the changes between 2000 and 2100 due to all forcings, b) the changes between 2000 and 2100 due to increasing GHG concentrations and c) the changes between 2000 and 2100 due to declining ODS levels for June (when the ozone mass flux is maximum in the NH and minimum in the SH; see Fig. 2a). Significant changes on the 95%-confidence level are colored. The black dotted line represents the mean tropopause position in the REF2000 simulation. For the small ODS-induced changes (c) additional contour lines (2, 3, and 4 ppbv) are shown.



1087

1088

1089

1090

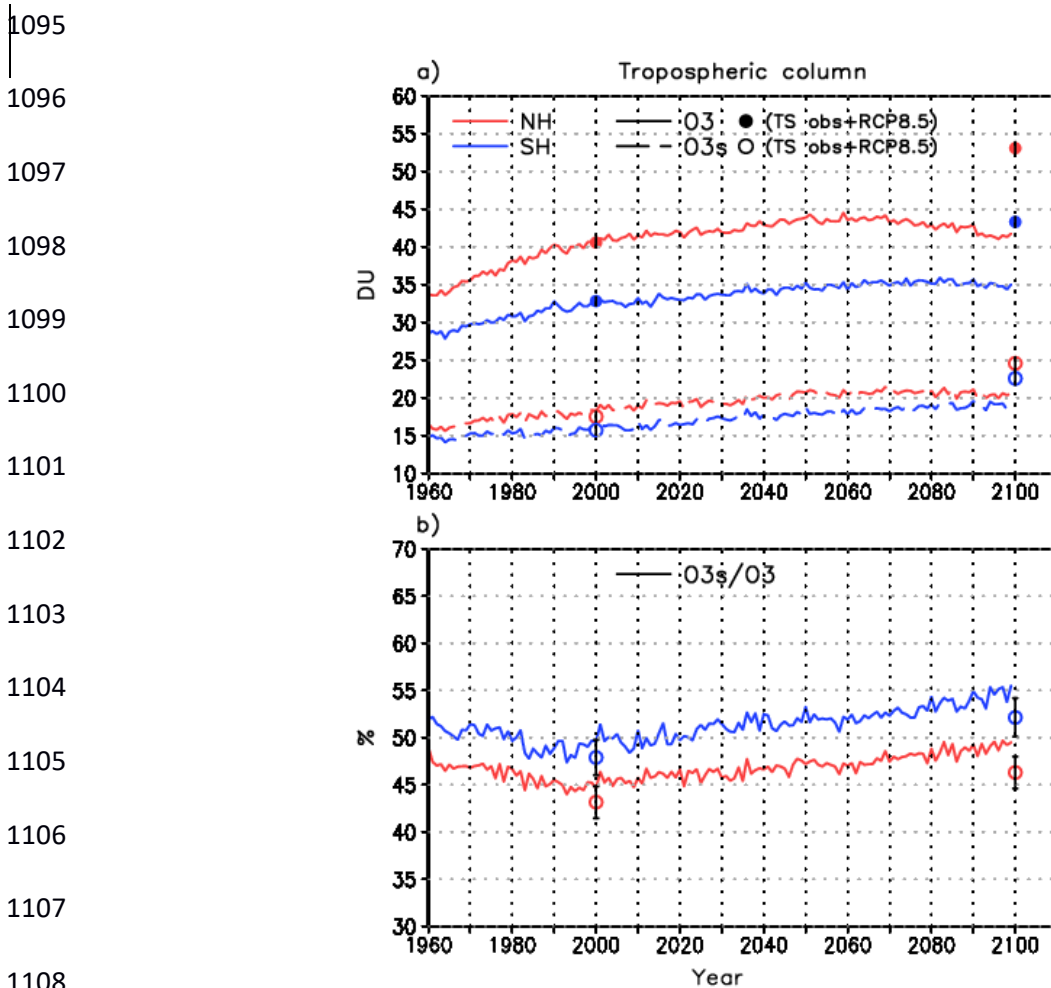
1091

1092

1093

1094

Figure 9: As Figure 6, but for the change in the tropospheric columns of O_3 [DU] (upper row), the tropospheric columns of O_{3s} [DU] (middle row), and the contribution of the O_{3s} changes to the O_3 changes between 2000 and 2100 [%] (bottom). The small numbers at the top of the figures are the respective annual mean global mean changes in DU and %. Shading in the bottom row indicates the regions where both, O_{3s} and O_3 changes, are significant on the 95% confidence level.



1100 **Figure 109:** a) Temporal evolution of the annual mean tropospheric column in ozone (solid)
 1111 and O3s (dashed) [DU] averaged for the NH (red) and the SH (blue) in the transient RCP6.0
 1112 simulation and the corresponding values of the reference timeslice simulations for the year 2000
 1113 and 2100 (ozone: closed circle; O3s: open circle). b) Same as a) but for the ratio between O3s
 1114 and O3 [%]. The black bars denote the $\pm 2\sigma$ range for the timeslice simulations. Note that the
 1115 interannual variability in ozone and O3s is small in the timeslice simulations and the error
 1116 bars are very short.

1117